Southeastern Geology: Volume 36, No. 3 November 1996

Editor in Chief: S. Duncan Heron, Jr.

Abstract

Academic journal published quarterly by the Department of Geology, Duke University.

SOUTHEASTERN GEOLOGY

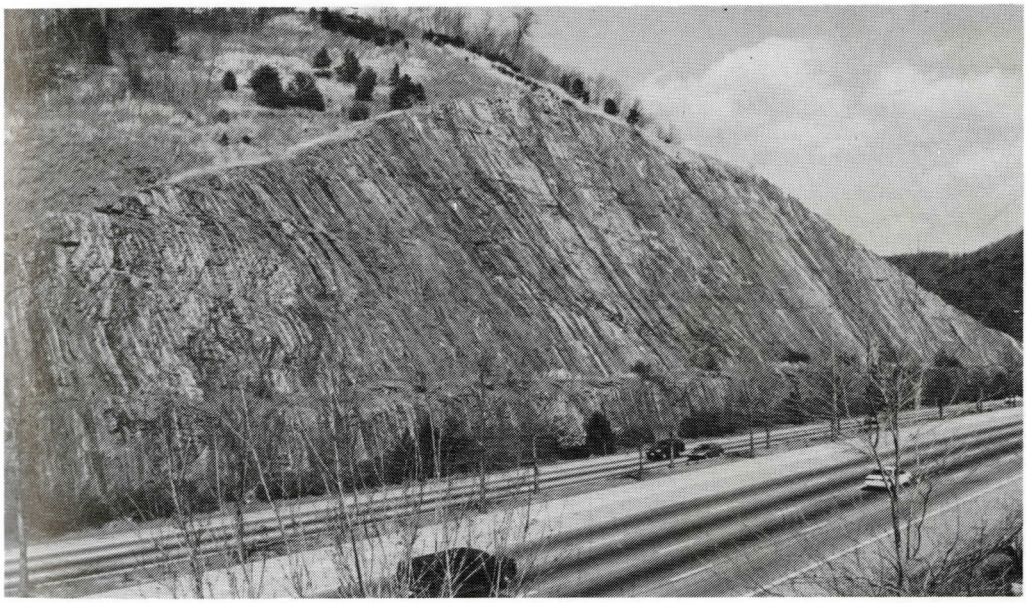

VOL. 36, NO. 3 NOVEMBER 1996

SOUTHEASTERN GEOLOGY

PUBLISHED

at

DUKE UNIVERSITY

Editor in Chief:

Duncan Heron

This journal publishes the results of original research on all phases of geology, geophysics, geochemistry and environmental geology as related to the Southeast. Send manuscripts to **DUNCAN HERON, DUKE UNIVERSITY, BOX 90233, DURHAM, NORTH CAROLINA 27708-0233**. Phone: 919-684-5321, Fax: 919-684-5833, Email: heron@geo.duke.edu Please observe the following:

1) Type the manuscript with double space lines and submit in duplicate.
2) Cite references and prepare bibliographic lists in accordance with the method found within the pages of this journal.
3) Submit line drawings and complex tables reduced to final publication size (no bigger than 8 x 5 3/8 inches).
4) Make certain that all photographs are sharp, clear, and of good contrast.
5) Stratigraphic terminology should abide by the North American Stratigraphic Code (American Association Petroleum Geologists Bulletin, v. 67, p. 841-875).

Subscriptions to *Southeastern Geology* for volume 36 are: individuals - $17.00 (paid by personal check); corporations and libraries - $22.00; foreign $26. Inquires should be sent to: **SOUTHEASTERN GEOLOGY, DUKE UNIVERSITY, BOX 90233, DURHAM, NORTH CAROLINA 27708-0233**. Make checks payable to: *Southeastern Geology*.

Information about SOUTHEASTERN GEOLOGY is now on the World Wide Web including a seachable author-title index 1958-1995. The URL for the Web site is:

http://www.geo.duke.edu/seglgy.htm

SOUTHEASTERN GEOLOGY is a peer review journal.

ISSN 0038-3678

SOUTHEASTERN GEOLOGY
V. 36, No. 3, November 1996, p. 99-122

A SURVEY OF THE MAJOR-ELEMENT GEOCHEMISTRY OF GEORGIA GROUNDWATER

L. BRUCE RAILSBACK[1], POLLY A. BOUKER[1], THOMAS P. FEENEY[2], ETHAN A. GODDARD[1], KEITH E. GOGGIN[1], A. SHAWN HALL[1], BRIAN P. JACKSON[3], ANGELA A. MCLAIN[1], MICHAEL C. ORSEGA[1], MARGARET A. RAFTER[1], AND JAMES W. WEBSTER[2]

[1]Department of Geology, University of Georgia, Athens, GA, 30602-2501
[2]Department of Geography, University of Georgia, Athens, GA, 30602-2502
[3]Department of Crop and Soil Science, University of Georgia, Athens, GA, 30602

ABSTRACT

Examination of 412 chemical analyses from throughout Georgia reveals that bedrock lithology, weathering systematics, physical hydrology, and mineral stability relationships control inter- and intra-regional trends in groundwater chemistry. As a result, Georgia's four geologic provinces have relatively distinct groundwater chemistries. However, flow through fractures and karst obscures chemical relationships of groundwater to lithology and depth, except in the Coastal Plain.

Chemical weathering driven by carbonic acid makes HCO_3^- the dominant anion of most Georgia groundwaters, even in regions devoid of carbonate rocks, and all four geologic provinces have at least some groundwaters that are supersaturated with respect to $CaCO_3$. Weathering reactions thus explain much of the variability of Georgia groundwaters except those in Coastal Plain carbonates, where diagenetic reactions involving unstable depositional phases lead to anomalously high concentrations of Mg^{+2} and dissolved silica. Another control on groundwater chemistry in at least the Blue Ridge and Piedmont appears to be equilibrium with kaolinite and, in some cases, smectite forming in soils.

Most of the major elements in Georgia groundwater do not pose health threats to human users. However, the relationships that emerge from studies like this one of the lithologic, hydrologic, and thermodynamic controls on groundwater chemistry should allow better prediction and characterization of groundwater as utilization of water resources increases in the coming decades.

INTRODUCTION

Human demands on water supplies have increased greatly in the last decade and, as a result, accurate characterization and prediction of groundwater chemistry have become increasingly important. The state of Georgia provides an interesting setting for the study of groundwater chemistry because of its broad range of geological and physiographic environments. The range of those environments, from the Appalachian Valley and Ridge to the Atlantic Coast, means that insights into Georgia groundwater chemistry should have application from Alabama to the Carolinas at the least.

Although there are hundreds of published chemical analyses of Georgia groundwaters, most surveys or interpretations have been made at the county or regional level (e.g., Cressler, 1963; Steele, 1987; Sprinkle, 1989). The few state-wide treatments of groundwater chemistry have either been qualitative (e.g., Kundell, 1978) or descriptive rather than interpretative (e.g., Sonderegger and others, 1978). This paper attempts to fill that gap by examining a large suite of major-element groundwater analyses from across Georgia. It also tests some of the accepted explanations of groundwater chemistry and tries to link geological, geochemical, and hydrological concepts in considering the controls on groundwater variability.

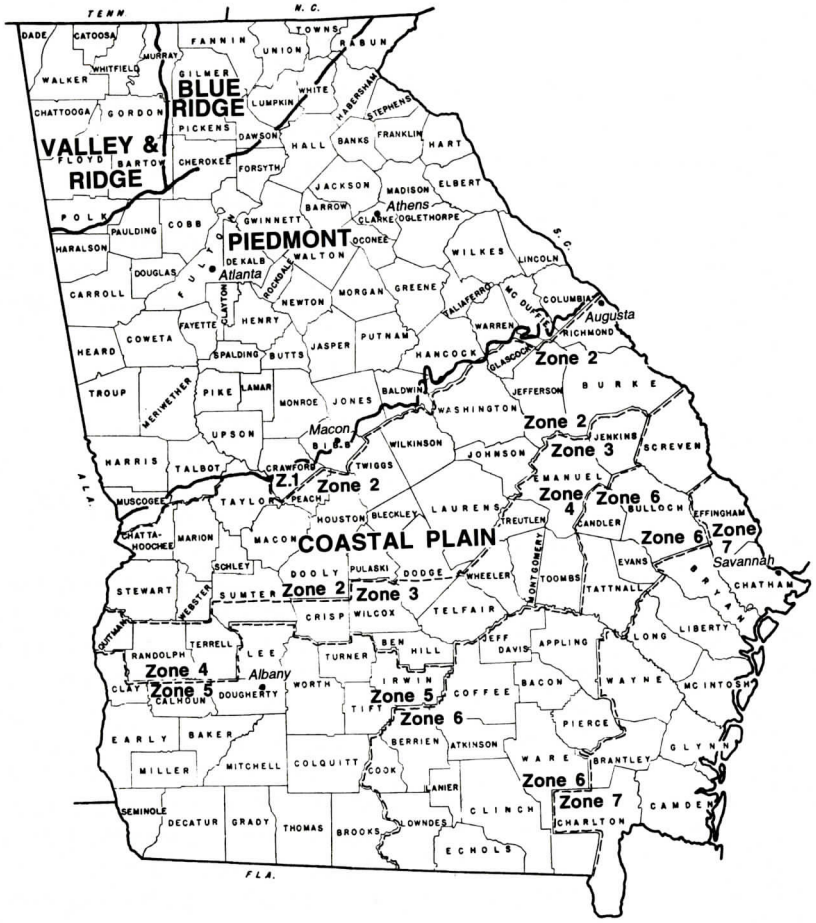

Figure 1. Map of Georgia showing the four geologic provinces described in the text. Dashed lines define numbered zones in southern Georgia that are used to identify samples on Figure 20. Zones 1, 2, and 3 are used for samples from Cretaceous siliciclastics and Zones 4, 5, 6, and 7 for samples from Tertiary carbonates, so Zone 3 overlaps with Zones 4, 5, and 6.

GEOLOGIC, PHYSIOGRAPHIC, AND HYDROLOGIC SETTING

Georgia is traditionally divided into four geologic provinces, the Valley and Ridge region in the northwest, the Blue Ridge in the north, the Piedmont in the north-central part of the state, and the Coastal Plain, which covers the southern half of the state (Figure 1). The Valley and Ridge, as its name implies, consists of NNE-SSW trending ridges and valleys underlain by Paleozoic sedimentary rocks folded and faulted during Late Paleozoic orogeny (Figure 2). The sedimentary rocks contain numerous carbonate units, including the Cambro-Ordovician Knox Dolostone and the Ordovician Chickamauga Limestone, and consequently caves and karst terrain are present across large parts of the Valley and Ridge. In the far northwest corner of the state, Pennsylvanian siliciclastics underlie what some authors have considered the Cumberland Plateau, but the continuity of lithology and deformation northwest all the way to the Sequatchie Thrust in Tennessee and Alabama leads us to include the entire region in the Valley and Ridge.

The Blue Ridge consists of metasediments and low-grade metamorphic rocks that are

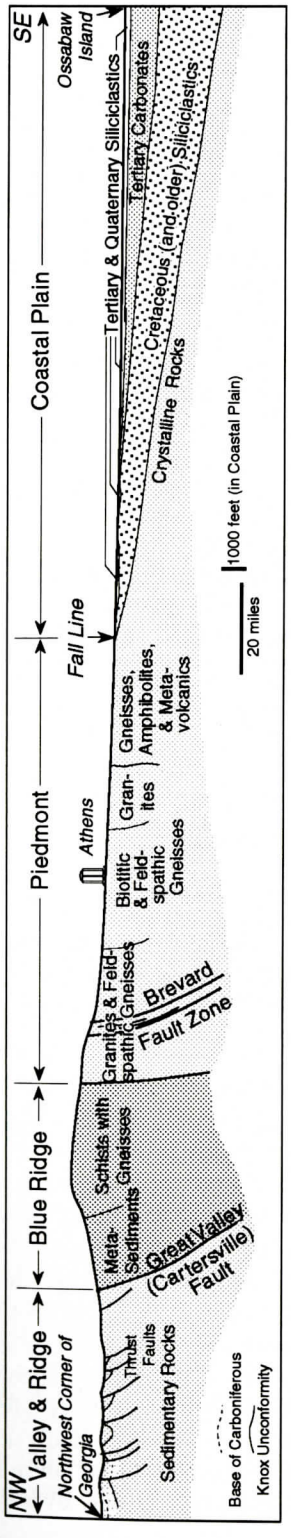

Figure 2. Schematic cross section from the northwest corner of Georgia to the Atlantic shoreline of Ossabaw Island. Orientations of, and in some cases existence of, faults in Blue Ridge and Piedmont are speculative. Constructed with information from geologic map of Georgia by Lawton, Marsalis, and others (1976) and cross section of the Coastal Plain of Georgia and South Carolina by Colquhoun and others (1991).

probably Proterozoic to Paleozoic in age. In contrast, the Piedmont is characterized by high-grade metamorphic rocks and igneous rocks, and compositions range from mafic amphibolites to felsic granites and granitic gneisses. The Blue Ridge, as its name implies, is generally an area of high relief, whereas the Piedmont largely consists of rolling hills and broad slopes dissected by stream valleys. The boundary we have used between the Blue Ridge and Piedmont is a lithologic one that follows faults and geologic contacts from Rabun County to Cherokee County (Figure 1). Other authors have, on the basis of other criteria, placed the boundary much further north, and at least one physiographic approach (Hodler and Schretter, 1986) extends the Piedmont to the Tennessee-Georgia state line. On the other hand, Williams (1978) placed the boundary further south than ours, along the Brevard fault zone from the South Carolina state line in Habersham County through northwest Atlanta and to Heard County on the Alabama state line.

The Coastal Plain lies south of the Piedmont and south of the Fall Line, a line of barriers to navigation on Georgia's major rivers at which the cities of Columbus, Macon, Milledgeville, and Augusta developed. The Coastal Plain is underlain by Mesozoic and Cenozoic sedimentary rocks that decrease in age toward the coast. Cretaceous siliciclastic rocks and overlying Tertiary limestones are the principal sources of groundwater in the Coastal Plain, and the latter are targets of wells from Americus and Albany in southwest Georgia to Savannah and Brunswick on the Atlantic coast (Figure 2). The Tertiary carbonates grade updip into calcareous Clayton and Claiborne sands.

A variety of names, many of them overlapping, have been used for water-bearing rock units in the Coastal Plain (Figure 3). We have tried to simplify that complexity by grouping our samples into those from Cretaceous siliciclastics (including the Providence and Midville aquifers), those from Tertiary carbonates (including the locally sandy Clayton and Claiborne aquifers, as well as the Floridan and Principal Artesian aquifer systems and the Oca-

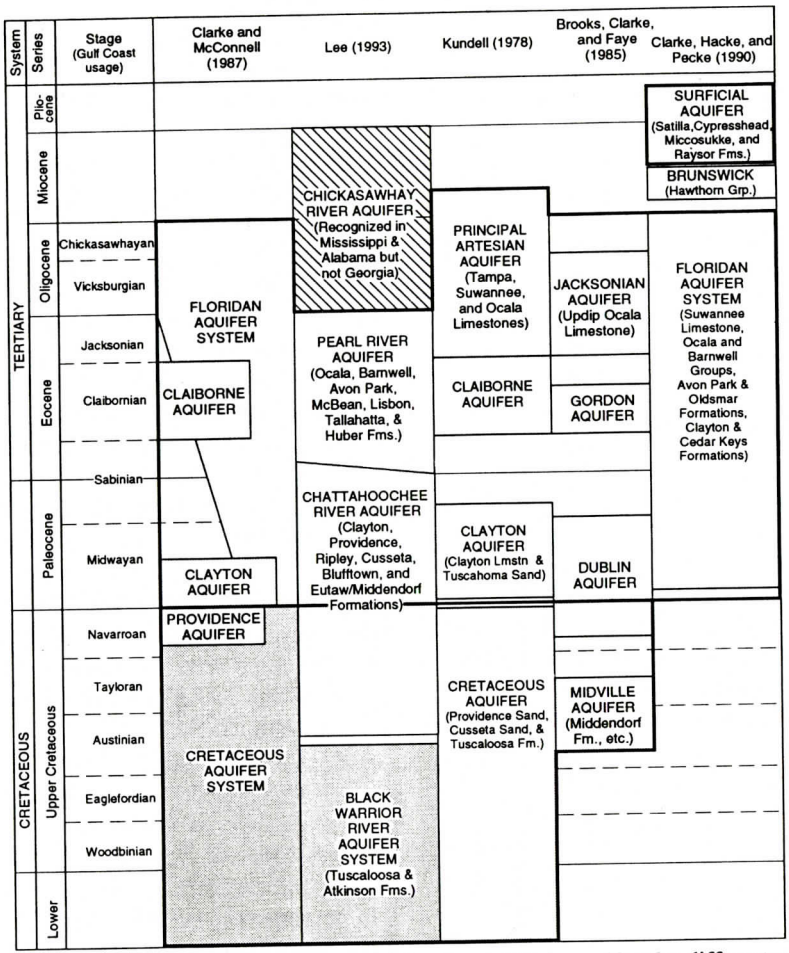

Figure 3. Chart showing different terminology used for Coastal Plain aquifers by different authors. Thick lines outline groups of aquifers (Cretaceous siliciclastics, Tertiary carbonates, and surficial siliciclastics) discussed in text. Stringfield (1966) provides a history of the nomenclature of the Tertiary carbonate aquifers, and Sprinkle's (1989) Figure 5 shows nomenclatural changes in what he calls the "Floridan aquifer system". For extension into South Carolina, see Figure 2 of Lee and Strickland (1988).

la Limestone), and those from surficial aquifers, including Miocene and Pliocene strata near the Atlantic coast (Figures 2 and 3).

Average annual rainfall across the state ranges from 45 to 70 inches (114 to 178 cm), but in exceptionally dry years rainfall can drop to as low as 30 inches (76 cm) in southern Georgia, and in wet years it can exceed 85 inches (216 cm) in far northern Georgia (Hodler and Schretter, 1986). Rainfall exceeds evapotranspiration across the state on an annual basis. Most regions, however, experience a water deficit in the summer (Hodler and Schretter, 1986), and in some summers water supplies for human use reach critically low levels.

Groundwater provides more than 60% of the water used by humans in the Coastal Plain, and intense withdrawal in coastal counties has led to pronounced cones of depression and saltwater intrusion (Krause and Randolph, 1989; Clarke and McConnell, 1987). Groundwater accounts for less than 30% of the total water consumed in the northern half of the state (Hodler and Schretter, 1986), but use of groundwater there is expected to increase in the near future as surface supplies become increasingly overuti-

Table 1. Average Compositions of Shallow (<700 ft) Groundwaters

			Coastal Plain		
	Valley & Ridge	Blue Ridge	Piedmont	Siliciclastics	Carbonates
Ca^{+2}	38.6	12.2	16.3	9.9	39.4
Mg^{+2}	9.2	2.1	3.4	1.5	10.7
Na^{+}	11.9	3.7	26.4	12.9	17.4
K^{+}	1.5	1.7	2.1	1.5	1.9
HCO_3^{-}	163.4	49.3	53.5	51.5	152.4
SO_4^{-2}	13.7	4.4	13.0	3.5	31.9
Cl^{-}	5.7	2.0	37.5	6.3	16.5
F^{-}	0.16	0.16	0.20	0.21	0.26
SiO_2	12.4	16.3	30.4	13.7	27.7
TDS	183.6	73.0	168.0	87.0	229.4
pH	7.3	6.5	6.8	6.3	7.7

All values except pH are ppm (mg/L)

lized and subject to contamination. Groundwater use increased 420% in Georgia between 1950 and 1980, and the rate of groundwater withdrawal for the entire state now exceeds 1 billion gallons per day (Davis and Turlington, 1987).

DATA AND METHODS

The data used in this paper are from 412 previously published chemical analyses of Georgia groundwaters made between 1938 and 1991, although most date from the 1960s and 1970s. This range of ages of analyses is only slightly greater than that used by Sprinkle (1989) in his definitive study of the Floridan aquifer system. The data used in this paper include 77 analyses from the Valley and Ridge, 39 from the Blue Ridge, 138 from the Piedmont, and 158 from the Coastal Plain. Data density is greatest in the Valley and Ridge, where surface lithology varies over short distances, but the 412 wells include at least one from each of the state's 159 counties.

The data are a non-random sample of published chemical analyses. Analyses were excluded because of missing data, apparent pollution, and excessive age, whereas other analyses were preferentially included to broaden the distribution with respect to geography, depth, and bedrock lithology. High imbalance of charge was used to eliminate faulty analyses, but some analyses with charge imbalance in excess of 10% were kept in the data set because application of a uniform limit would preferentially eliminate shallow, low-TDS samples for largely computational reasons and thus would lead to a biased data set.

Almost all analyses include the parameters listed in Table 1, and some include Fe, Sr^{+2}, and NO_3^{-} concentrations as well. Wherever possible, measured (rather than calculated) TDS values were used. Very few of the publications from which the data were taken indicate the sampling procedures and analytical techniques used, but the range of ages of the analyses suggests a variety of procedures and techniques (see Sprinkle, 1989, p. I-25). As a result, disparities undoubtedly exist in the data, but a t-test of pH values (which are highly sensitive to method) that were measured before and after 1969 shows no statistically significant difference ($p=0.33$). (The choice of 1969 as the break point for this test is dictated by Sprinkle's (1989) review of methods used in groundwater analyses in the southeast). Copies of the data set used in this paper are available on request from the authors.

Saturation of samples with respect to cal-

cite and dolomite was calculated two ways. One technique involved a spreadsheet in which activity coefficients were calculated using the extended Debye-Hückel equation and the Davies equation, and saturation states were calculated using $\log K_{sp} = -8.48$ for calcite and $\log K_{sp} = -17$ for dolomite. The second approach was to use MINTEQA2 (Allinson and others, 1991), a geochemical speciation program that models the equilibrium speciation of a solution, including ion pair formation (e.g., $CaHCO_3^-$ and $CaSO_4^0$) and precipitation of oversaturated phases. Despite the greater sophistication of the MINTEQA2 approach, the results were nearly the same for both methods.

STATE-WIDE COMPARISONS AND TRENDS

Results

The most general observation that we can make is that Georgia's four geologic provinces do exhibit significant differences in groundwater chemistry. For example, pH and concentrations of total dissolved solids (TDS), Ca^{+2}, Mg^{+2}, and HCO_3^- are greatest in the Valley and Ridge and Coastal Plain, the two sedimentary provinces, and are least in the Blue Ridge (Figure 4).The same regional distribution holds for degree of saturation with respect to calcite (Figure 5). On the other hand, concentrations of dissolved silica (reported here as $SiO_{2(aq)}$) are greatest in the Piedmont and Coastal Plain and least in the Valley and Ridge (Figure 6 and Table 1). Concentrations of dissolved silica show the greatest range in groundwaters less than 500 feet deep, where waters are supersaturated with respect to both quartz and chalcedony (Figure 6). In contrast, groundwaters at depths greater than 1300 feet show a narrow range that is nearer, but still above, equilibrium with quartz.

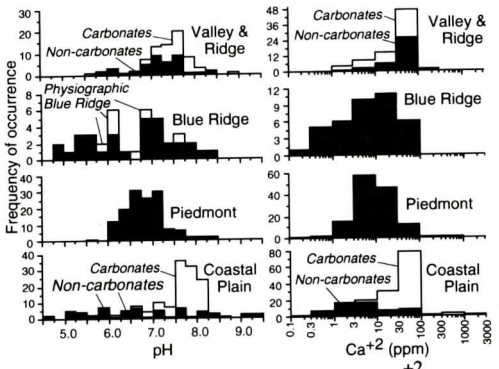

Figure 4. Histograms showing pH and Ca^{+2} concentrations of groundwaters from different geologic provinces of Georgia. Note that scales for both sets of histograms are logarithmic and that vertical scales vary.

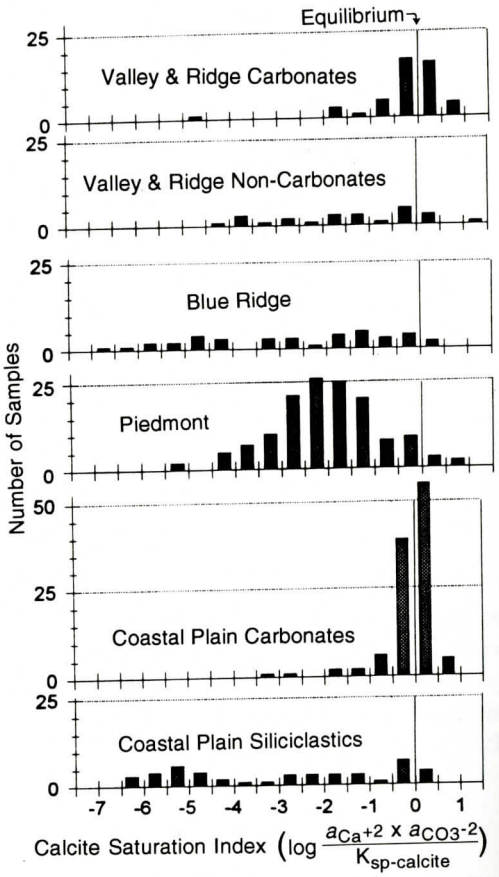

Figure 5. Histograms showing calcite saturation index of Georgia groundwaters. Results are from spreadsheet calculations described in text and are supported by MINTEQA2 calculations.

The Piedmont is the only region in which a majority of samples (69%) have greater molar Na^+ concentrations than Ca^{+2} concentrations, and only in the Piedmont and in groundwaters from Coastal Plain siliciclastics does the aver-

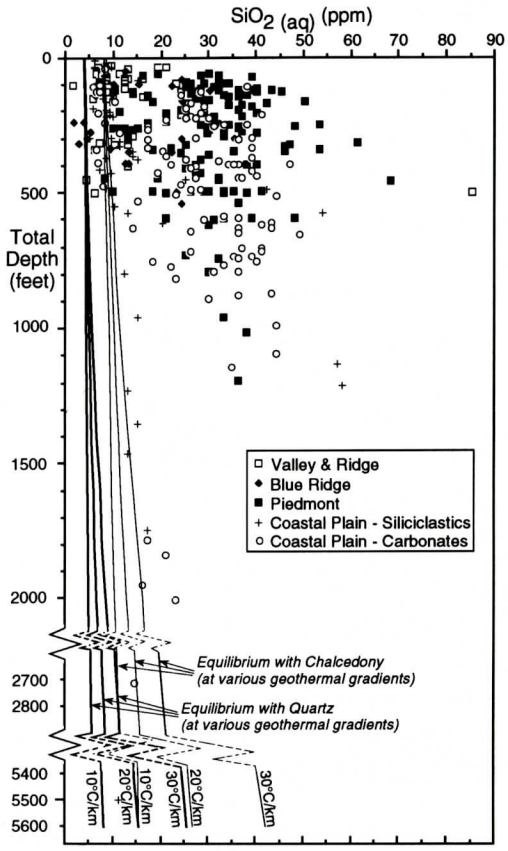

Figure 6. Plot of $SiO_{2(aq)}$ concentrations as a function of total depth of well. Note condensed vertical scale at bottom of diagram. Equilibrium with quartz (dark lines) and chalcedony (lighter lines) (as indicated by Figure 1B of Williams and Crerar 1985) is shown assuming geothermal gradients ranging from 10°C/km to 30°C/km (the range of geothermal gradients in Georgia reported by Kron and Stix (1982) and Kron and others (1991)). Equilibrium with amorphous silica is offscale to right, so all samples are undersaturated with respect to amorphous silica.

age Na^+ concentration exceed that of Ca^{+2} by weight (Table 1). If we subdivide Coastal Plain groundwaters into those hosted by siliciclastics versus those in Tertiary carbonate aquifers, the resulting five provincial groups show statistically significant differences in $SiO_{2(aq)}$ and HCO_3^- concentrations (Table 2), except for the comparison of groundwaters from the Blue Ridge and Coastal Plain siliciclastics.

Differences between the regions can also be seen on a modified Piper diagram (Figure 7), where Valley and Ridge samples generally cluster as Ca-Mg-HCO_3-rich waters. Piedmont and Blue Ridge samples similarly cluster in the Ca-Mg-HCO_3 region, but have a broader distribution. Coastal Plain samples are distributed across the entire diagram and thus include Na–K-rich waters and SO_4–Cl-rich waters. Most of the latter, however, are from deep wells that introduce considerable diversity to the data set.

The relationship of chemical parameters to depth also varies between the four provinces. Correlation of TDS with depth is very weak in the Piedmont and Valley and Ridge, and weak in the Blue Ridge (Table 3). It is also weak in the Coastal Plain if the latter is considered as a whole. However, correlation of TDS with depth is much stronger if one considers the groundwaters from the Cretaceous siliciclastics and Tertiary carbonates separately. The same statements generally apply to the correlation of pH with depth, except that pH and depth show essentially no correlation at all in Tertiary carbonates of the Coastal Plain.

Despite these correlations (or lack thereof) between TDS and depth and pH and depth, pH and TDS show a striking positive correlation across the state (Figure 8). Low pH and low TDS generally characterize shallow samples, whereas high pH and high TDS tend to be more common in deeper samples. The only significant outliers to this trend are two shallow Coastal Plain samples that are rich in NO_3^- and some very deep high-TDS samples from the Coastal Plain, including some from the Atlantic Coast that probably are influenced by seawater infiltration. Other parameters with significant relationships to pH include NO_3^-, which is most abundant in shallow, low-pH, samples and is scarce in both high pH samples and deep samples (Figure 9).

Despite the differences between regions, constant relative abundances of cations and anions emerge from examination of shallow samples from across the state. For example, in wells less than 700 feet deep all across the state, Ca^{+2} is the most abundant cation (by molar concentration) in 54% of the samples. In fact, Georgia groundwater chemistry is sufficiently consis-

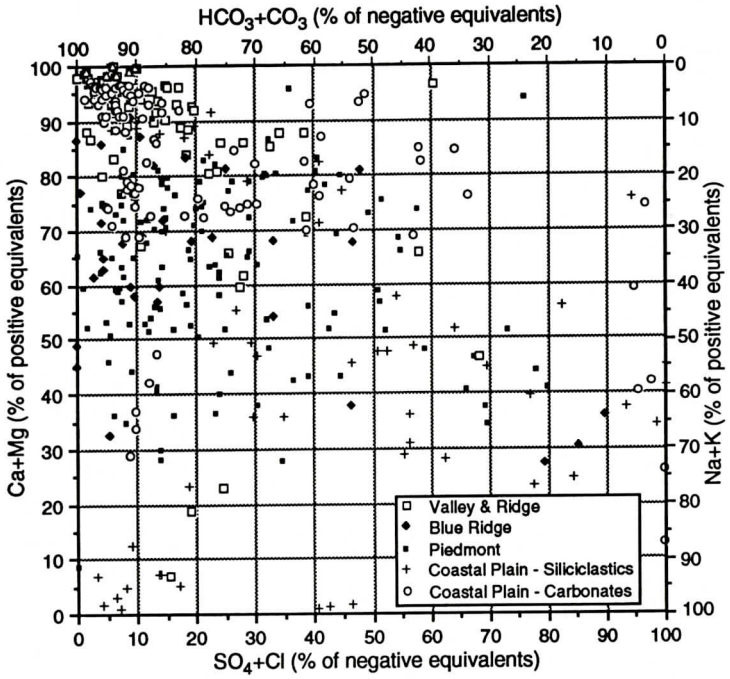

Figure 7. Modified Piper Diagram (Piper, 1953) showing compositions of Georgia groundwaters by equivalents. Coastal Plain groundwaters are the most diverse in their compositions, whereas Valley and Ridge groundwaters are the most tightly clustered in the Ca-Mg-HCO_3-CO_3 corner.

Table 2. Statistical significance[a] of differences between means of concentrations of dissolved silica (upper right) and HCO_3^- (lower left) in Georgia groundwaters.

				Coastal Plain	
	Valley & Ridge	Blue Ridge	Piedmont	Siliciclastics	Carbonates
Valley & Ridge	-	ns[b]	<0.001	0.04	<0.001
Blue Ridge	<0.001	-	<0.001	ns[b]	<0.001
Piedmont	<0.001	<0.001	-	<0.001	0.02
C.P. Sili'ics	<0.001	ns[b]	0.015	-	<0.001
C.P. Carbonates	0.04	<0.001	<0.001	<0.001	-

[a] Statistical significance expressed as *p*, the probability that the observed differences would have arisen randomly. Thus p=0.015 for HCO_3^- in the Piedmont and in Coastal Plain siliciclastics indicates a 1.5% chance that the difference between those groups arose randomly. Results are from two-tailed t-tests on log-transformed data.

[b] "ns" = not significant.

tent that the relation of molar concentrations Ca>Na>Mg>K holds in 25% of all samples and in 28% of samples from wells between 100 and 500 feet deep (about five to seven times the proportion that would be expected to arise randomly). In wells less than 700 feet deep, HCO_3^- is the most abundant anion in 89% of the samples, and it is the most abundant anion in 93% of all wells in the Piedmont, despite that region's lack of carbonate rocks. Cl^- molality exceeds that of F^- in 96% of all samples and in 99% of all samples from the Coastal Plain, and the order of molal concentrations HCO_3>Cl>SO_4>F holds in 45% of all samples (about ten times the proportion that would be expected to arise randomly).

Table 3. Correlation of TDS with total depth of wells.

Province	r^2 for TDS	r^2 for pH
Valley & Ridge	0.049	0.046
Valley & Ridge (Carbonates Only)	0.085	0.071
Blue Ridge	0.217	0.167
Piedmont (all)	0.005	0.031
Piedmont (excluding one well)	0.050	0.037
Coastal Plain (all)	0.194	0.060
Coastal Plain (Cretaceous siliciclastics only)	0.564	0.167
Coastal Plain (Eocene carbonates only)	0.474	0.004

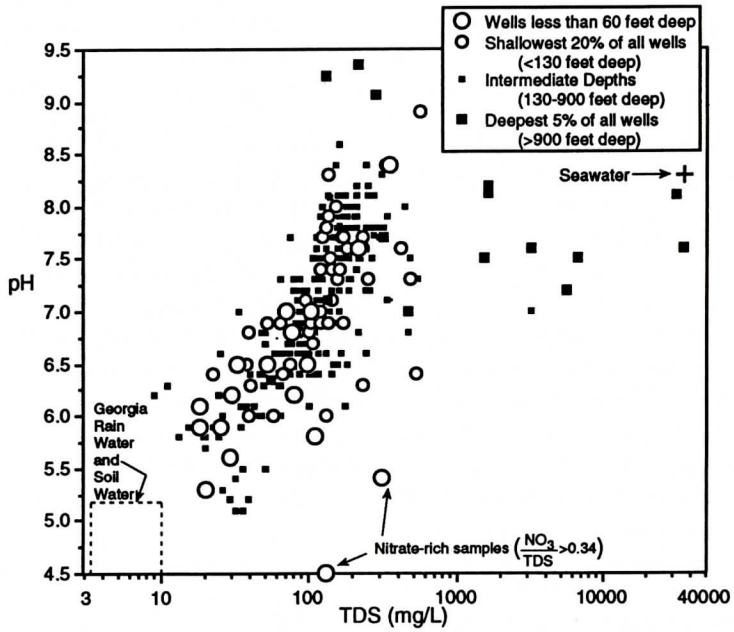

Figure 8. Variation of pH with TDS for all samples from all regions. Nitrate-rich samples are labeled because nitrate contamination, unlike mineral weathering, contributes to TDS without buffering low pH.

Discussion

From a state-wide perspective, the frequency of groundwaters in which molar concentrations have the relative abundance Ca>Na>Mg>K is explained by the similar average abundance of those elements in the continental crust, where Ca≈Na>Mg>K (Table 22-1 of Krauskopf, 1979). On the other hand, F is 8.5 times as abundant as Cl in the continental crust, and the reversal of their abundances in groundwater must be attributed to the much greater abundance of Cl than F in rainwater (a result of seawater chemistry), the faster release of Cl than F in weathering (Wanty and others, 1992) and to the generally greater solubility of Cl-bearing minerals.

The supersaturation of nearly all samples with respect to quartz presumably reflects the kinetic inhibition of quartz nucleation and precipitation, and the solubility of other silicates, especially clay minerals. In the case of those samples at or below equilibrium with respect to quartz, the very deep samples may have had sufficient time to approach equilibrium, whereas very shallow samples have probably not dissolved enough silicates to reach or significantly exceed equilibrium with respect to quartz.

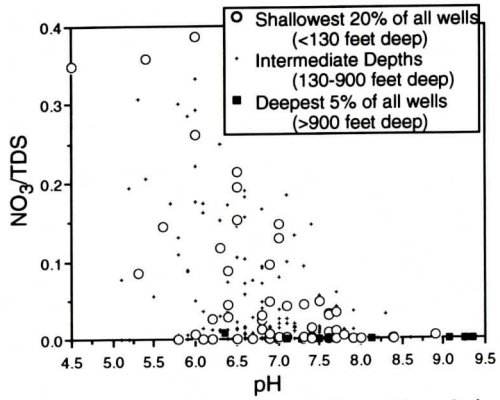

Figure 9. Relationship between pH and the relative abundance of NO_3^- in all dissolved solids, for all samples with NO_3^- data from all regions. All NO_3^--rich samples are samples with low pH, and many are shallow samples as well. Absolute NO_3^- concentrations in shallow samples are as great as 109 ppm, whereas all deep (>900 feet) samples have low NO_3^- concentrations less than 7 ppm.

The abundance of HCO_3^- in all regions, and especially in the Piedmont, points to the importance of weathering reactions in which carbonic acid reacts with silicate minerals to produce dissolved cations, clays, dissolved silica, and bicarbonate. The carbonic acid originates from the dissolution of atmospheric and soil CO_2 in groundwaters. Bicarbonate accumulates as carbonic acid dissociates whereas the hydrogen ions resulting from this dissociation are consumed in weathering reactions. Table 4 provides some examples of these weathering reactions, which are the key to neutralization of both natural and anthropogenic acids in soil waters and groundwater (Appelo and Postma, 1994, p. 223-226; White and Brantley, 1995). The weathering reactions listed in Table 4 produce dissolved solids as they neutralize the acidity of carbonic acid, and thus they also illustrate why pH and TDS correlate positively in Figure 8. Thus the diagonal trend in Figure 8 illustrates the maturation of acidic, dilute shallow soil water to buffered, more concentrated groundwaters at greater depths.

The relationship of pH to NO_3^- (Figure 9) is another example in which pH serves as an indicator of the maturity of groundwater. Shallow NO_3^--rich samples lose their NO_3^- through time and with increasing depth, probably to bacterial processes (Lovley and Chapelle, 1995; Stumm and Morgan, 1981; p. 453-461) (although it is possible that the NO_3^--rich samples simply reflect anthropogenic pollution of relatively young and thus shallow groundwaters).

Armed with the model of CO_2-driven weathering and resultant pH change as a measure of groundwater evolution, we now consider the different provinces of Georgia individually.

Table 4. Some Typical Reactions in Chemical Weathering.

Mineral	Weathering Reaction	HCO_3^-/SiO_2
Olivine	$4H_2CO_3 + MgFeSiO_4 \rightarrow Mg^{+2} + Fe^{+2} + 4HCO_3^- + SiO_{2(aq)} + 2H_2O$	4:1
Pyroxene	$4H_2CO_3 + MgFe(SiO_3)_2 \rightarrow Mg^{+2} + Fe^{+2} + 4HCO_3^- + 2SiO_{2(aq)} + 2H_2O$	2:1
Amphibole	$14H_2CO_3 + (MgFe)_7Si_8O_{22}(OH)_2 \rightarrow 7(Mg,Fe)^{+2} + 14HCO_3^- + 8SiO_{2(aq)} + 8H_2O$	1.75:1
Anorthite	$2H_2CO_3 + 2CaAl_2Si_2O_8 + H_2O \rightarrow 2Ca^+ + 2HCO_3^- + Al_2Si_2O_5(OH)_{4(s)}$	∞
Plagioclase (An_{50})	$6H_2CO_3 + 2CaNaAl_3Si_5O_{16} + 3H_2O \rightarrow 2Ca^+ + 2Na^+ + 6HCO_3^- + 3Al_2Si_2O_5(OH)_{4(s)} + 4SiO_{2(aq)}$	1.5:1
K Feldspar	$2H_2CO_3 + 2KAlSi_3O_8 + 1H_2O \rightarrow 2K^+ + 2HCO_3^- + Al_2Si_2O_5(OH)_{4(s)} + 4SiO_{2(aq)}$	1:2
Quartz	$SiO_{2(s)} \rightarrow SiO_{2(aq)}$ ($SiO_{2(s)} + 2H_2O \rightarrow H_4SiO_{4(aq)}$)	0:1

PIEDMONT AND BLUE RIDGE

Results

Piedmont and Blue Ridge groundwaters have some of the lowest pH values in the state. The bimodal distribution of pH in the Blue Ridge (Figure 4) might prompt the hypothesis that a more restrictive definition of "Blue Ridge" as only the high-relief regions of northernmost Georgia would yield a population of groundwaters with very low pH. However, the lowest pH values (<5.0) actually are found in groundwaters from Cherokee County in the southern Blue Ridge, and groundwaters from the northernmost counties have pH values that, although low, are not exceptionally low within the Piedmont and greater Blue Ridge (Figure 4).

Within the Piedmont, pH values and TDS vary subtly with lithology. Groundwaters sampled from more "weatherable" (Drever and Clow, 1995) mafic bedrock (amphibolites, hornblende gneisses, and metamafics) tend to have higher pH and TDS than groundwaters from felsic rocks (granites and granitic gneisses) (Fig 10a). This mafic/felsic distinction is weak but can also be seen if one uses Mg/K and HCO_3^-/SiO_2 ratios as indices of mafic character (Figure 10b). The former of these ratios simply reflects the abundance of cations in mafic and felsic rocks. The latter ratio arises from Table 4, which shows that stoichiometry dictates higher HCO_3^-/SiO_2 ratios in the dissolved products of weathering of minerals that are higher in Bowen's Reaction Series. Within the mafic rocks of the Piedmont, the mean HCO_3^-/SiO_2 ratio of groundwaters from hornblende gneisses (3.97) is greater than that of groundwaters hosted by amphibolites (2.10), and the mean Mg/K ratio of groundwaters from hornblende gneisses (3.44) is greater than that of groundwaters hosted by amphibolites (2.23). (The difference in HCO_3^-/SiO_2 ratios is statistically significant (p=0.01), but the difference in Mg/K ratios is not). Thus groundwaters from hornblende gneisses seem to have a more "mafic" character than those from amphibolites.

Mineral stability diagrams also show some

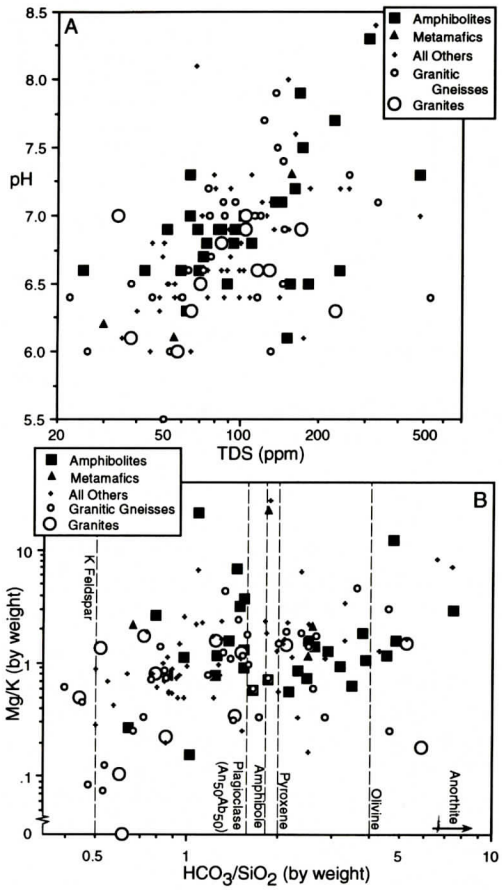

Figure 10. Plots of chemistry of Piedmont groundwaters, with symbols indicating bedrock lithology; note that darker symbols are for more mafic lithologies. A. Plot of pH and total dissolved solids (TDS). B. Plot of weight ratios of HCO_3^- and $SiO_{2(aq)}$ concentrations and of weight ratios of Mg^{+2} and K^+ concentrations in Piedmont groundwaters. Ratios are constructed to maximize mafic characteristics at upper right of diagram and felsic tendencies at lower left, as suggested by Table 4.

segregation of groundwaters from mafic and felsic rocks. For example, Figure 11 shows stability relationships in the system CaO-Al_2O_3-SiO_2-H_2O and shows that Piedmont and Blue Ridge groundwaters range from compositions compatible with equilibrium with gibbsite to kaolinite to Ca-beidellite, a smectite. Nonetheless, groundwaters from mafic rocks have higher SiO_2 concentrations and $Ca^{+2}/(H^+)^2$ ratios, whereas groundwaters from siliceous rocks, es-

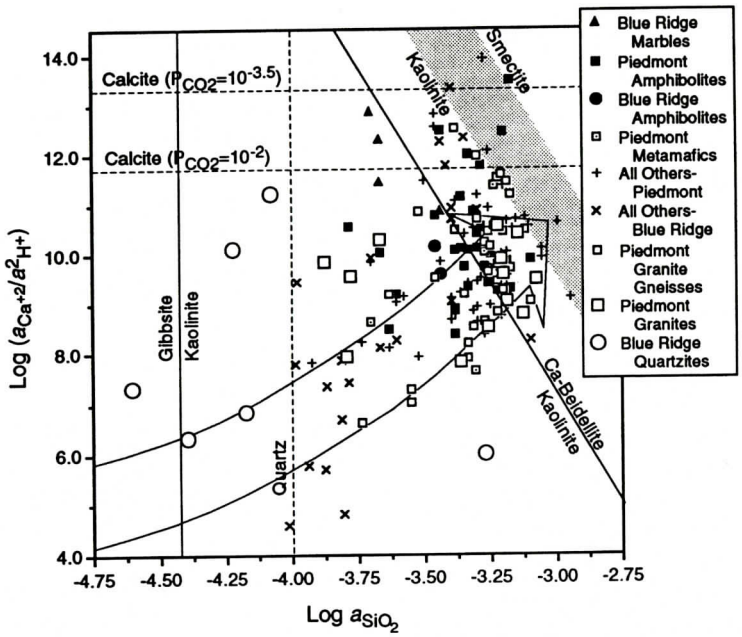

Figure 11. Mineral stability diagram comparing chemistry of Blue Ridge and Piedmont groundwaters with groundwater compositions in equilibrium with gibbsite, kaolinite, and Ca-beidellite (a smectite) in the system $CaO\text{-}Al_2O_3\text{-}SiO_2\text{-}H_2O$. Open symbols are for groundwaters from felsic rocks and dark ones for groundwaters from mafic rocks; circles are for Blue Ridge samples and squares are for Piedmont samples. Large open arrow shows expected evolution of groundwater chemistry with weathering from acidic low-TDS condition to equilibrium with minerals. Equilibrium lines are from Figure 6-9 of Drever (1988), except for shaded kaolinite-smectite boundary from Jones and Bowser (1978); large open arrow is from Figure 9.8b of Stumm and Morgan (1981).

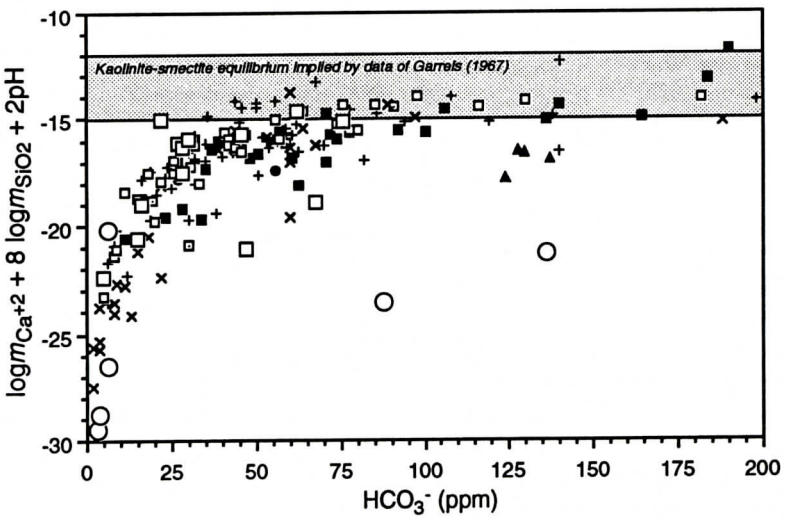

Figure 12. Kaolinite-smectite reaction index of Garrels (1967) of Piedmont and Blue Ridge groundwaters (vertical axis) plotted against HCO_3^- concentration. Constancy of index at HCO_3^- concentrations greater than 75 ppm suggests an approach to equilibrium between kaolinite and smectite. Symbols are same as in Figure 11.

pecially quartzites, have the opposite characteristics. The kaolinite-smectite reaction index values (Garrels, 1967) of these groundwaters also approach apparent kaolinite-smectite equilibrium, and the groundwaters from mafic rocks plot nearest that equilibrium (Figure 12).

Most Piedmont and Blue Ridge groundwaters are undersaturated with respect to calcite (Figure 5). However, MINTEQA2 results show that four of our 39 Blue Ridge samples are saturated or supersaturated with respect to calcite, and only two of those samples come from marble host rock. Six of our 138 Piedmont samples are at least saturated with respect to calcite, and the Piedmont has no carbonate-bearing rocks at all. The host rocks of the calcite-saturated samples include three hornblende gneisses, an amphibolite, three gneisses, and one cataclastic unit in addition to the two marbles mentioned above. Those samples are from Bartow, Cherokee, White, Cobb, Elbert, Fulton, Gwinnett, and Monroe Counties.

Discussion

Figures 10 and 11 show that bedrock lithology has *some* influence on groundwater chemistry in the Piedmont and Blue Ridge, in that more mafic rocks tend to generate groundwaters rich in Ca^{+2}, Mg^{+2}, and HCO_3^- compared to groundwaters hosted by felsic rocks. However, the data show that there is little consistency to back up previous claims of "large differences in constituent concentrations... between wells deriving water from granitic (light) rocks and mafic (dark) rocks" (Cressler and others, 1983). In river waters, chemical composition can be clearly linked to igneous and metamorphic bedrock lithologies of watersheds (as is shown by the data in Table 2 of Bricker and Jones (1995)), but this linkage is much less consistent in the waters hosted by crystalline rocks of the Piedmont and Blue Ridge. The inconsistency of the results could be due to the variable and poorly mapped bedrock geology of the Blue Ridge and especially the Piedmont, where low relief and dense vegetation have hindered geologic mapping. However, the failure of chemical parameters to correlate with depth (Table 3), combined with the weak relationships of chemistry to lithology, suggests that much of the irregularity of groundwater chemistry in the Piedmont and Blue Ridge may be because fracture flow allows groundwaters to move vertically and across lithologies. Fractures can provide pathways for significant groundwater flow to depths as great as 500 feet in the Piedmont and Blue Ridge (Stewart, 1962). This allows water to react with one lithology but to be recovered from another lithology at depth, and a fracture high in a well may yield much of that well's water far above the well bottom (see, for example, LeGrand, 1967). Thus the physical hydrology of the Piedmont and Blue Ridge, where fractures allow flow through rocks that are otherwise essentially impermeable, can impart great apparent heterogeneity and unpredictability to groundwater chemistry.

The lower pH values found in the Blue Ridge as compared to the Piedmont probably reflect a variety of factors. More mafic lithologies in the Piedmont may buffer acidity more effectively, but the thicker soils of the Piedmont and resulting increased weathering rates (Drever and Clow, 1995) may also allow more buffering, regardless of lithology, than in Blue Ridge soils (as one might infer from the work of Chen and others, 1984). In addition, the generally higher rainfall in the Blue Ridge than in the Piedmont may cause a more water-dominated system in which weathering fails to buffer acidity.

The use of mineral stability diagrams to interpret groundwater chemistry merits many caveats, because many clay minerals are still not well characterized thermodynamically (e.g., Drever, 1988, p. 112-114) *and* because the assumption of thermodynamic equilibrium may be unwarranted in many weathering environments (Allard, 1995, p. 152). Nonetheless, Figure 11 suggests that many groundwaters are in equilibrium with kaolinite, as might be expected from the abundance of kaolinite-group minerals in Georgia soils (Melear, 1990). Perhaps more surprising is the compatibility of many groundwater compositions with equilibrium

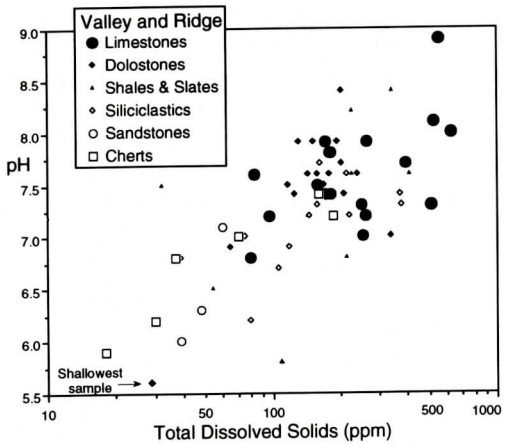

Figure 13. Plot of pH and TDS of Valley and Ridge groundwaters. Symbols indicate host lithology; lighter symbols indicate more chemically inert lithologies. Groundwaters in carbonate rocks plot in high-pH, high-TDS region, whereas groundwaters in silica-rich rocks plot in low-pH, low-TDS region. The most striking exception is the shallowest sample, in which the groundwater has probably not reached equilibrium with its dolomitic host rock.

with smectite, a clay mineral generally expected in more arid climates. However, Barshad's (1966) work on clay minerals developed on various igneous terrains in California showed that smectites persist in areas of relatively high rainfall if the bedrock is mafic. In addition, Velbel (1985) found that smectite occurs in North Carolina at the base of kaolinite-rich saprolites, where low water-rock ratios cause little flushing of cations, and Kantor and Schwertmann (1974) similarly found smectites deep in soils below overlying kaolinitic horizons. These observations, plus the Eocene production of smectite in the Piedmont to generate the smectitic Twiggs Clay (Huddleston and Hetrick, 1986), show that the abundance of samples from mafic rocks in the smectite field in Figure 11 is not as anomalous as the wet Georgia climate might suggest.

Another seeming anomaly might be the presence of groundwaters saturated with respect to calcite in humid regions of crystalline rocks. Some of the saturated Piedmont samples are from what are now the most populous counties in Georgia, raising the possibility of human contamination, but the depths of the wells, the low populations at the times the wells were sampled, and the saturation of groundwaters from igneous rocks elsewhere (Garrels, 1967) all suggest that the observed calcite saturation is natural. Furthermore, calcite precipitated at low temperatures in fractures in Precambrian igneous and metamorphic rocks elsewhere (Frape and others, 1992) and calcite supersaturation in granitic groundwaters (Waber and Nordstrom, 1992) illustrate that groundwaters in such rocks commonly reach calcite saturation. The abundance of HCO_3^--rich groundwaters and the scattering of groundwaters that are saturated with respect to calcite point out the significance of CO_2-driven weathering reactions. The fact that four of ten calcite-saturated samples are from mafic rocks further illustrates the production of HCO_3^- in the weathering of mafic minerals shown in Table 4.

VALLEY AND RIDGE

Results

The geochemistry of Valley and Ridge

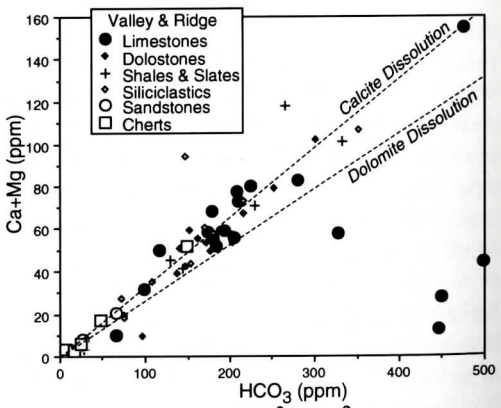

Figure 14. Plot of $Ca^{+2}+Mg^{+2}$ and HCO_3^- concentrations (by weight) of Valley and Ridge groundwaters. Dashed diagonal lines indicate compositions that would result from dissolution of nothing but stoichiometric calcite and dolomite (dissolution of Mg calcites and Ca-rich dolomites would generate compositions between the two lines). Symbols indicate host lithology; lighter symbols indicate more chemically inert lithologies.

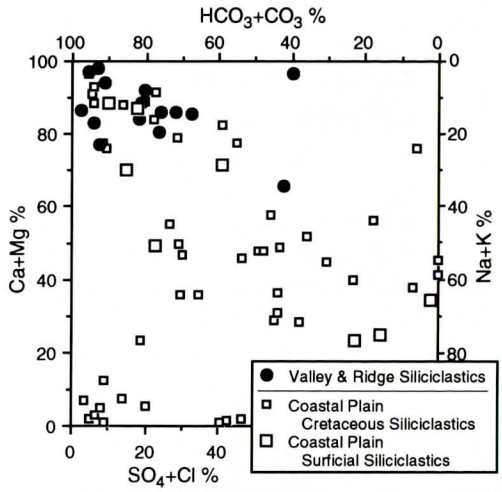

Figure 15. Modified Piper Diagram (Piper, 1953) showing compositions of groundwaters in siliciclastic rocks in the Valley and Ridge and Coastal Plain. "Siliciclastics" in this figure includes "siliciclastics" and "sandstones" in Figures 13 and 14. Groundwaters in Coastal Plain siliciclastics are much more chemically diverse than those in Valley and Ridge siliciclastics.

groundwaters varies with host lithology more distinctly than do groundwaters in the Piedmont and Blue Ridge, but considerable overlap in chemistries nonetheless exists. In general, chemically inert, silica-rich, rocks like cherts and sandstones host groundwaters with pH values of 5.5 to 7.5 and with TDS less than 200 ppm, whereas more reactive carbonate rocks host groundwaters with pH values of 7.0 to 9.0 and TDS greater than 70 ppm (Figure 13). Groundwaters from cherts and sandstones generally have low Ca^{+2}, Mg^{+2}, and HCO_3^- concentrations compared to those from carbonate rocks (Figure 14). However, if one considers the range of chemistries possible from pure calcite dissolution and pure dolomite dissolution, most groundwaters from all lithologies fall within those bounds, so that most groundwater chemistry, regardless of host lithology, is compatible with dissolution of carbonate rocks or fracture-filling carbonate minerals (Figure 14). The only major exceptions to that generalization are three samples from the Chickamauga Limestone that have anomalously high HCO_3^- and Na^+ concentrations. In fact, many Valley and Ridge groundwaters are supersaturated with respect to calcite, including some groundwaters from non-carbonate host rocks (Figure 5).

The compatibility of Valley and Ridge groundwaters with carbonate dissolution is also reflected in the predominance of Ca-Mg-HCO_3 groundwaters, as opposed to Na-K-SO_4-Cl groundwaters, as shown in Figure 7. The extent of the dominance of Ca-Mg-HCO_3 groundwaters can be seen by comparing groundwaters from Valley and Ridge siliciclastics (the "siliciclastics" and "sandstones" of Figures 13 and 14) with groundwaters from Coastal Plain siliciclastics. Despite the similarity of the lithologies, Coastal Plain siliciclastics host groundwaters with a broad range of chemistries, but Valley and Ridge siliciclastics host a much narrower range of groundwaters dominated by Ca^{+2}, Mg^{+2}, and HCO_3^- (Figure 15).

Ca^{+2}, Mg^{+2}, and HCO_3^- so dominate the geochemistry of Valley and Ridge groundwaters that seemingly little other significant variation exists. If one considers the other potentially significant ions, the only noticeable trend is that shales, slates, and siliciclastics tend to be rich in SO_4^{-2} relative to Cl^- (Figure 16). This may be the result of pyrite oxidation. No similar trend exists in Fe^{+2} abundance, probably because most Fe from pyrite oxidation is oxidized and

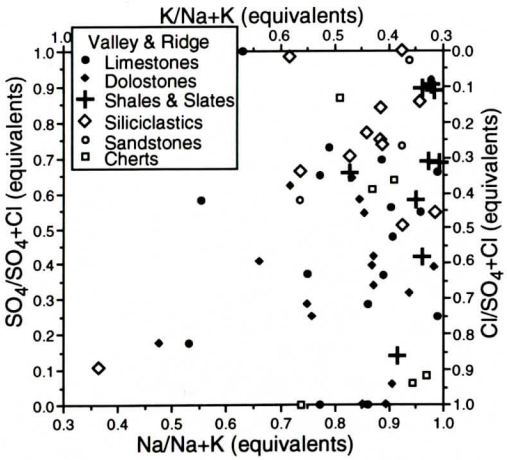

Figure 16. Na-K-SO_4-Cl compositions of Valley and Ridge groundwaters by equivalents (a derivative of a Piper diagram). Symbols indicate host lithologies.

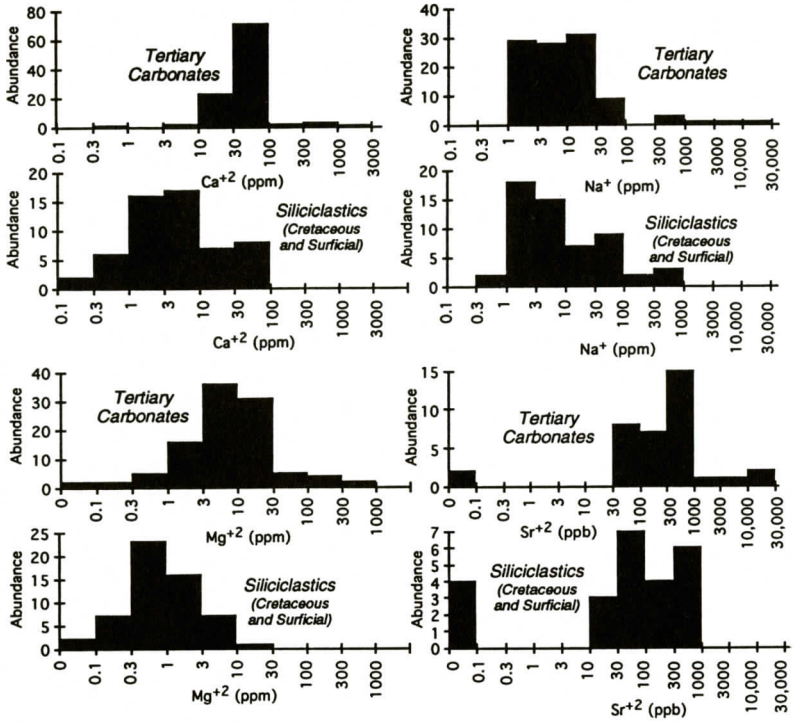

Figure 17. Histograms showing concentrations of Ca^{+2}, Mg^{+2}, Na^{+}, and Sr^{+2} in Coastal Plain carbonate and siliciclastic aquifers. Note logarithmic horizontal scales.

precipitated from groundwaters as oxides and hydroxides. Unlike Piedmont groundwaters, most Valley and Ridge groundwaters fall in the kaolinite stability field of the CaO-Al_2O_3-SiO_2-H_2O system.

Discussion

The dominance of Ca-Mg-HCO_3 groundwaters in the Valley and Ridge and the compatibility of most Valley and Ridge groundwaters with calcite and/or dolomite dissolution suggests that most groundwaters interact with carbonate rocks, regardless of the host lithology from which they are sampled. This widespread dominance of carbonate chemistry, combined with the failure of chemical parameters to correlate with depth (Table 3), implies that flow of groundwaters through discrete strata-bound aquifers does not account for the observed chemical variability. Despite the presence of sedimentary strata in the Valley and Ridge, the data are more compatible with flow across aquifers. Fractures probably account for much of the cross-formational flow, and karst developed in the region's many limestones contributes to vertical water movement that allows groundwaters to reach considerable depths without significant water-rock interaction (White, 1988).

COASTAL PLAIN

Results

Unlike the Valley and Ridge, Blue Ridge, and Piedmont, the Coastal Plain is characterized by groundwater chemistries that vary distinctly with host lithology. Ca^{+2} and Mg^{+2} concentrations are generally greater in the Tertiary carbonate system than in the Cretaceous and surficial siliciclastics, although the two groups show little difference in Na^{+} and Sr^{+2}, especially if one discounts high concentrations of these cations in exceptionally deep carbonate samples (Figure 17). Most groundwaters from

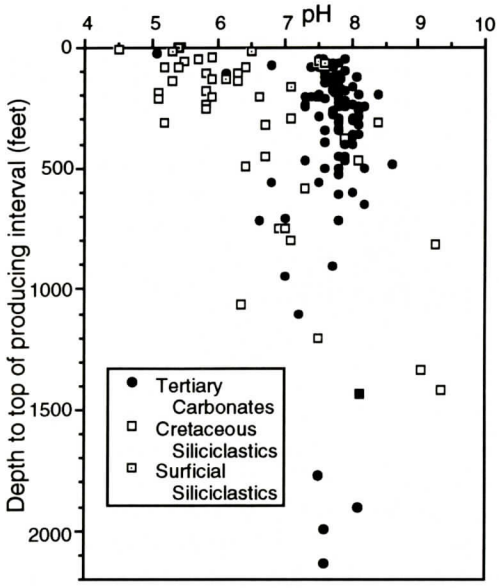

Figure 18. Plot of variation of pH of Coastal Plain groundwaters with depth of the top of the producing interval. Note uniformity of pH of all but the shallowest samples in carbonate aquifers (filled circles) but increasing pH with depth of samples from siliciclastic aquifers (squares).

Tertiary carbonates are saturated with respect to calcite, whereas groundwaters from siliciclastics are generally undersaturated (Figure 5), and the same is true for dolomite saturation. pH values in Tertiary carbonates are nearly all between 6.5 and 8.5 and show little variation with depth, except for low near-surface values, whereas pH values in Cretaceous and surficial siliciclastics vary from 4.5 to 9.5 and increase with depth (Figure 18).

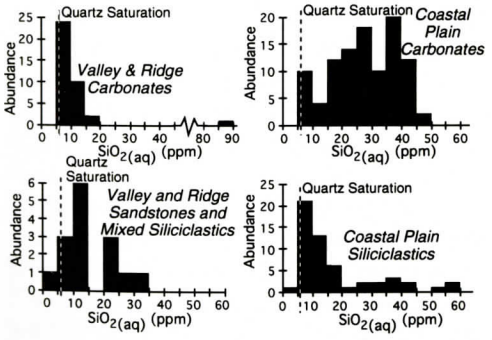

Figure 19. Histograms of concentrations of dissolved silica in groundwaters hosted by siliciclastic rocks and carbonate rocks in the Coastal Plain and Valley and Ridge. Concentrations of dissolved silica are high in Coastal Plain carbonates compared both to those in other carbonates and those in siliciclastics.

In addition to the above differences, $SiO_{2(aq)}$ concentrations are generally higher in groundwaters from Tertiary carbonates than in those from the siliciclastics (Figure 19). Comparison with Valley and Ridge groundwaters shows that not all groundwaters in carbonate rocks have high $SiO_{2(aq)}$ concentrations, and thus the high concentrations in groundwaters from Coastal Plain carbonates are an anomaly with respect both to the Coastal Plain and to carbonates in general.

Geographic variation exists in groundwaters from both siliciclastics and carbonates. Samples from Cretaceous siliciclastics nearest the Piedmont derive at least 40% of their negative charge from SO_4^{-2} and Cl^-, whereas samples furthest from the Piedmont derive no more than 50%, and generally less than 20%, of their negative charge from those anions (Figure 20). Samples from Tertiary carbonates that are dominated by Ca^{+2}, Mg^{+2}, and HCO_3^- occur all across the Coastal Plain, but the only samples with nearly all of their negative charge from SO_4^{-2} and Cl^- are from near the Atlantic coast, and the only samples with most of their negative charge from HCO_3^- and most of the positive charge from Na^+ and K^+ are from the southwestern Coastal Plain (Figure 20). One coincidence of these trends is that groundwaters from Dougherty, Calhoun, Quitman, Clay, and Lee Counties in southwest Georgia are Na-K-HCO_3-rich, regardless of their host rocks. Figure 5 shows that some groundwaters in Coastal Plain carbonates are undersaturated with respect to calcite. Although many of those groundwaters are in or near Dougherty County, most are scattered across the Coastal Plain in all four of the zones shown on Figure 1.

Although deep groundwaters in the Valley and Ridge, Blue Ridge, and Piedmont are all HCO_3^--rich, many deep groundwaters in Coastal Plain carbonates are rich in SO_4^{-2} and Cl^-. Samples from carbonates more than 1320 feet (400 m) deep are rich in either SO_4^{-2} or Cl^-,

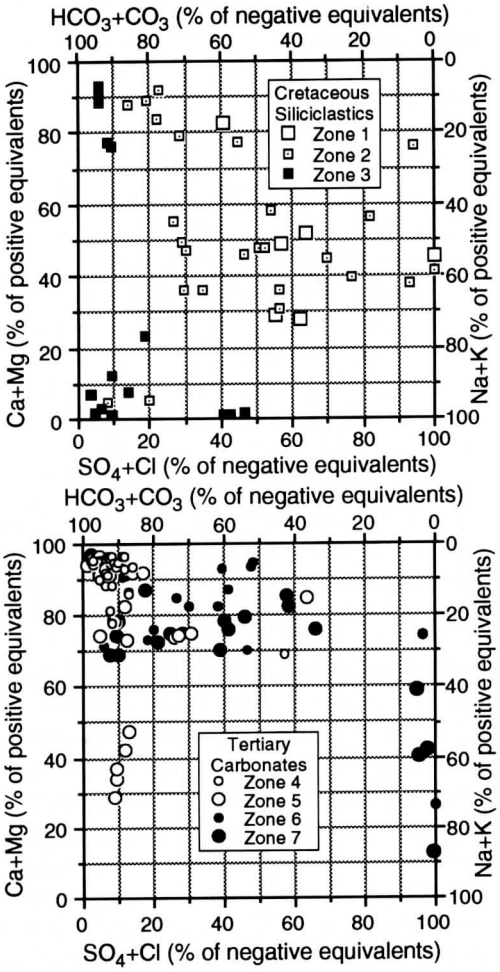

Figure 20. Modified Piper diagrams (Piper, 1953) showing geographic variation in groundwaters in Coastal Plain siliciclastics (above) and carbonates (below). Geographic zones are shown on Figure 1, where Zones 1, 2, and 3 extend from the Fall Line into the Coastal Plain and Zones 4, 5, 6, and 7 range from the interior of the Coastal Plain to the Atlantic Coast.

whereas those from siliciclastics are HCO_3^--rich and strikingly SO_4^{-2}-poor (Figure 21). SO_4^{-2} concentrations relative to TDS are low both compared to shallower groundwaters in Coastal Plain siliciclastics and compared to all Georgia samples (Figure 22), and the low SO_4^{-2} concentrations coincide with high pH values, as was the case with low NO_3^- concentrations (Figure 9). Groundwaters from both deep Coastal Plain carbonate and deep siliciclastics are increasingly Na^+-rich with increasing depth, as is typical of most deep brines, but the groundwaters from siliciclastics are consistently Mg^{+2}-poor compared to those from the carbonates (Figure 21). Thus the differentiation of groundwaters from carbonates and siliciclastics observed throughout the coastal plain is even more pronounced at extreme depth.

Discussion

The chemical differentiation of groundwaters hosted by different rock units in the Coastal Plain (Figures 17 to 19) points to the importance of flow within aquifers, rather than via fractures. The observed increase in pH and TDS with depth in Cretaceous siliciclastics also supports the notion of confined flow and further confirms the model of acidic groundwaters that are buffered and acquire dissolved solids with time. The failure of similar depth-dependence to emerge in carbonate units probably results in part from karstic flow through sinkholes, especially in the Dougherty Plain of southwest Georgia, and from the fast reaction of limestone to buffer natural acidity. Karstic flow probably also accounts for the broad geographic distribution of groundwaters undersaturated with respect to calcite.

Extensive calcite saturation and buffered pH values are expected in carbonate rocks rather than in siliciclastics, but the higher SiO_2 concentrations in groundwaters from Tertiary limestones than in groundwaters from Si-rich siliciclastics (Figure 19) are unexpected. The most likely source of this dissolved SiO_2 is dissolution of biogenic silica within the limestones. Marine sediments commonly contain amorphous biogenic silica that recrystallizes in a series of steps to ultimately yield diagenetic quartz. In deep sea sediments, amorphous silica phases can survive for as long as 120 million years and to depths of 1400 m (Hesse, 1988). Although the Coastal Plain provides a very different diagenetic environment than that encountered by deep-sea sediments, the comparison suggests that biogenic silica could still be

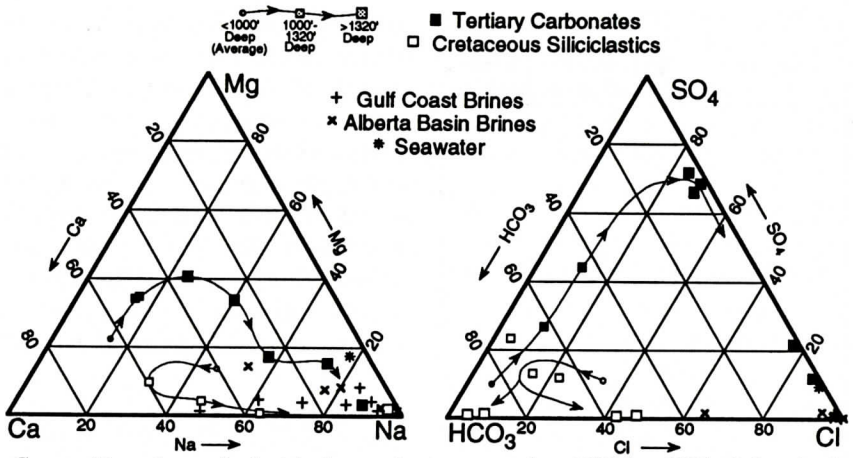

Figure 21. Compositions (by equivalents) of groundwaters more than 1000 feet (305 m) deep in the Coastal Plain, and compositions of seawater and brines elsewhere in North America for comparison. Smaller squares indicate samples 1000 to 1320 feet (305 to 400 m) deep; larger squares indicate deepest samples. Circles indicate average compositions of samples shallower than 1000 feet. Thin curves with arrows indicate general trends from shallow to deepest samples. Brine compositions are from Land and Macpherson (1992), Hanor (1987), and Connolly and others (1990).

present to generate the high $SiO_{2(aq)}$ concentrations, and Sprinkle (1989) indicates that opaline tests are rare but present in the Coastal Plain carbonates. In contrast, groundwaters in the much older Paleozoic limestones of the Valley and Ridge have low $SiO_{2(aq)}$ concentrations, presumably because any biogenic silica in those rocks has long since been altered to quartz.

Unlike $SiO_{2(aq)}$, Sr^{+2} concentrations in groundwaters from Tertiary carbonates that are hardly distinguishable from those in siliciclastics (Figure 17) probably reflect the shorter stabilization time of Sr-rich aragonite. Aragonite dissolution or stabilization commonly occurs over thousands to at most a few million years (e.g., Budd, 1988), so it is hardly surprising that Sr^{+2} derived from diagenetic alteration of aragonite to calcite is no longer recognizable in the carbonate groundwaters. Elevated Mg^{+2} concentrations in groundwaters from the carbonates may reflect the slower diagenetic stabilization of Mg-bearing calcites, which apparently takes place in a multi-step process involving "tens to hundreds of recrystallizations" (Budd and Hiatt, 1993). Although the timing of that process is still poorly constrained, the slow dissolution of many skeletal Mg-calcites (Walter, 1985; Turner and others, 1986) and slow precipitation of dolomite as a sink for Mg^{+2} make it plausible that the high Mg^{+2} concentrations may reflect the late stages of "early diagenesis" of biogenic Mg-calcites. Burt's (1993) mass-balance calculations suggested that dissolution of Mg-calcites plays an important role in the chemistry of groundwaters in the Upper Floridan Aquifer in the Savannah area.

Although most of the deep (>1000 feet) samples do not have the TDS levels characteristic of brines, the relative abundances of their cations approach those of the brines found deep in many sedimentary basins (Figure 21). Lee and Strickland (1988) and Lee (1993) attributed much of that cation variation to Ca-for-Na exchange with clays and to neoformation of Na-bearing smectites. The increase in relative abundance of Na^{+} certainly provides little evidence for albitization of Ca-bearing feldspars in Coastal Plain siliciclastics, despite the importance of that process in the Gulf Coast (Land and Milliken, 1981).

The anion systematics of the deep groundwaters are unlike those of most deep brines, in that the deep samples hosted by siliciclastics are dominated by HCO_3^{-} rather than Cl^{-}, and the samples from carbonates are dominated by SO_4^{-2} except where seawater infiltration has led

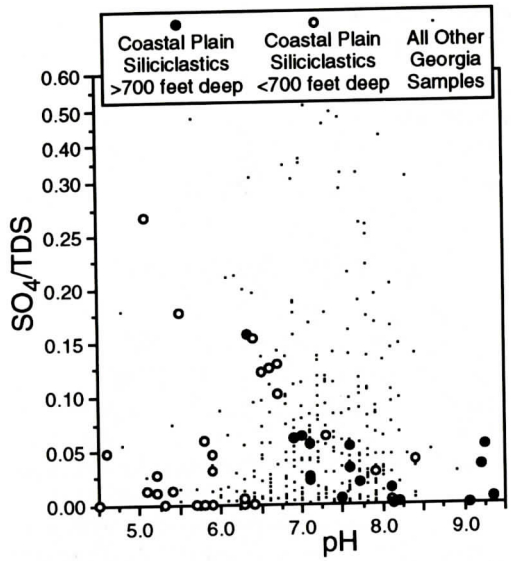

Figure 22. Relationship between pH and the relative abundance of SO_4^{-2} in all dissolved solids in groundwaters from Coastal Plain siliciclastics (large symbols) and all other Georgia groundwater samples (small symbols). Note the similarity of this plot to Figure 9. Absolute SO_4^{-2} concentrations in shallow samples are as great as 13 ppm, whereas all deep (>700 feet) samples have low NO_3^- concentrations less than 9 ppm. Note change in vertical scale at SO_4/TDS=0.30.

to Cl-rich compositions. The HCO_3^--rich groundwaters in the siliciclastics presumably reflect reaction with carbonic acid. The dearth of SO_4^{-2} in those samples probably reflects the activity of sulfate-reducing anaerobic bacteria in the deeper parts of the confined siliciclastic aquifers (Lovley and Chapelle, 1995). The lower SO_4^{-2} concentrations with increasing pH (Figure 22) illustrate the evolution of groundwater at depth in confined aquifers, in contrast to the less well defined relationship of pH and SO_4^{-2} concentrations in other aquifers.

The SO_4^{-2}-rich groundwaters in deep carbonates (Figure 21) are more enigmatic. Many hypotheses have been proposed for the origins of brines in sedimentary basins, including membrane filtration by shales, surface evaporation and infiltration of brines, expulsion of evaporite porewaters, subsurface dissolution of evaporites, and diagenetic alteration of shales, sandstones, and limestones (for a review, see Hanor, 1983). Subsurface dissolution of gypsum or anhydrite is the only likely explanation that can account for the observed SO_4^{-2}-rich compositions in Coastal Plain carbonates, because other scenarios involving seawater or evaporites would have introduced a Cl-rich brine more like those observed in the Gulf Coast or Alberta Basins. Sprinkle (1989) indicated that gypsum is "an important minor mineral" in the Coastal Plain carbonate aquifers.

PRINCIPAL CONCLUSIONS

1. Georgia's four geologic provinces have distinct groundwater chemistries, because of the different lithologies present and perhaps because of different rainfalls and different soil development. Any one analysis may fail to provide a clear indication of its region of origin, but there are clear differences between the groups of groundwaters from the four regions (or five "regions", if one separates groundwaters from siliciclastic and carbonate aquifers in the Coastal Plain).

2. Physical hydrology has a major influence on the vertical and lateral variation in groundwater chemistry. In the Valley and Ridge, Blue Ridge, and Piedmont, karstic flow and fracture flow allow little vertical differentiation of groundwaters, and in the Coastal Plain both lateral and vertical differences in groundwater chemistry in Tertiary carbonate aquifers are diminished by flow through karstic features. Vertical and lateral differences are best developed in the confined Cretaceous siliciclastic aquifers, where diffuse flow seems to be dominant.

3. The chemical evolution of shallow groundwaters is dominated by weathering reactions driven by carbonic acid. As a result, most groundwaters derive the bulk of their negative charge from HCO_3^-, and pH and TDS increase together as the result of sustained contribution of CO_2 from the atmosphere and soil processes (Figure 8). Production of HCO_3^- in these weathering reactions leads to saturation of at least

some groundwater samples with respect to calcite in all four regions, including the Piedmont (Figure 5).

4. Within regions, groundwater chemistry is partly controlled by bedrock lithology (Figures 10, 13, and 17). However, lithologic control is obscured to varying degrees in the Valley and Ridge, Blue Ridge, and Piedmont by movement of groundwaters through fractures, whereas lithologic influence is most evident in the Coastal Plain. In most regions, chemical relationships to lithology follow what would be considered weathering reactions, but in Coastal Plain carbonate aquifers Mg^{+2} and $SiO_{2(aq)}$ concentrations seem to reflect diagenetic reactions expected in carbonate sediments.

5. Many Piedmont and Blue Ridge groundwaters, especially those hosted by mafic lithologies, approach or are at kaolinite-smectite equilibrium (Figures 11 and 12), despite the observed abundance of kaolinite in the soils of those regions and despite Georgia's wet climate.

6. Cation relationships in deep Coastal Plain groundwaters approach those typical in deep brines found in sedimentary basins. However, relative anion abundances in groundwaters from siliciclastic host rocks reflect carbonic acid reactions and microbial sulfate reduction, and some groundwaters from Tertiary carbonates reflect gypsum dissolution and seawater infiltration.

7. Concentrations of dissolved silica exceed quartz equilibrium in nearly all groundwater samples (Figure 6), reflecting the slow precipitation kinetics of quartz. $SiO_{2(aq)}$ concentrations are highest in Piedmont groundwaters, where weathering of crystalline silicate rocks generates dissolved silica, and in groundwaters from Coastal Plain carbonates, where dissolution of biogenic silica may be important.

8. Groundwater chemistry shows remarkable variability, but the ranges of concentrations and geochemical behaviors outlined above permit recognition of natural, as opposed to anomalous and perhaps anthropogenic, major element chemistry. Given the increasing role of major element geochemistry in recognition of leachate contamination (Mirecki and Parks, 1994), this understanding of natural variability of major element chemistry should provide a background against which to compare new groundwater analyses as the search for and exploitation of groundwater continues and expands.

ACKNOWLEDGMENTS

We thank Jim McConnell of the U.S. Geological Survey for help in assembling the data set and for a thoughtful review of an early version the manuscript. We also thank Dr. John Dowd of the University of Georgia for his helpful comments, and Dr. Terri Woods of East Carolina University for a very helpful review of the manuscript.

REFERENCES CITED

Allard, B., 1995, Groundwater, in Salbu, B., and Steinnes, E., eds., Trace Elements in Natural Waters: Boca Raton, CRC Press, p. 151-176.

Allinson, J.D., Brown, D.S., and Novo-Gradac, K.J., 1991, MINTEQA2/PRODEFA2, a geochemical assessment model for environmental systems, Version 3.0: Athens, Georgia, Environmental Protection Agency, EPA/600/3091/021.

Apello, C.A.J., and Postma, D., 1994, Geochemistry, Groundwater and Pollution: Rotterdam, A.A. Balkema, 536 p.

Barshad, I., 1966, The effect of a variation in precipitation on the nature of clay mineral formation in soils from acid and basic igneous rocks: Proceedings of the International Clay Conference, Jerusalem, 1, p. 167-173.

Bricker, O.P, and Jones, B.F., 1995, Main factors affecting the composition of natural waters, in Salbu, B., and Steinnes, E., eds., Trace Elements in Natural Waters: Boca Raton, CRC Press, p. 1-20.

Brooks, R., Clarke, J.S., and Faye, R.E., 1985, Hydrogeology of the Gordon Aquifer system of east-central Georgia: Georgia Geological Survey Information Circular 75, 41 p.

Budd, D.A., 1988, Aragonite-to-calcite transformation during freshwater diagenesis of carbonates: Insights from porewater chemistry: Geological Society of America Bulletin, v. 100, p. 1260-1270.

Budd, D.A., and Hiatt, E.E., 1993, Mineralogical stabilization of high-magnesium calcite: geochemical evidence for intracrystal recrystallization within Holocene porcellaneous foraminifera: Journal of Sedimentary Petrology, v. 63, p. 261-274.

Burt, R.A., 1993, Ground-water chemical evolution and

diagenetic processes in the upper Floridan aquifer, southern South Carolina and northeastern Georgia: U.S. Geological Survey Water-Supply Paper 2392, 76 p.

Chen, C.W., Gherini, S.A., Peters, N.E., Murdoch, P.S., Newton, R.M., and Goldstein, R.A., 1984, Hydrologic analyses of acidic and alkaline lakes: Water Resources Research, v. 20, p. 1875-1882.

Clarke, J.S., Hacke, C.M., and Peck, M.F., 1990, Geology and ground-water resources of the coastal area of Georgia: Georgia Geological Survey Bulletin 113, 106 p.

Clarke, J.S., and McConnell, J.B., 1987, Georgia groundwater quality: U.S. Geological Survey Open-File Report 87-0720, 9 p.

Colquhoun, D.J., Arthur, M., Dillon, W.P., Hatcher, B., Huddlestun, P., Poag, C.W., Valentine, P.C., and Popenoe, P., 1991, Southeastern Atlantic Regional Cross Section - Eastern and Offshore South Carolina and Georgia Sector: American Association of Petroleum Geologists, 1:250,000.

Connolly, C.A., Walter, L.M., Baadsgard, H., and Longstaffe, F.J., 1990, Origin and evolution of formation waters, Alberta Basin, Western Canada Sedimentary Basin. I. Chemistry: Applied Geochemistry, v. 5, p. 375-395.

Cressler, C.W., 1963, Geology and ground-water resources of Catoosa County, Georgia: Georgia Geological Survey Information Circular 28, 19 p.

Cressler, C.W., Thurmond, C.J., and Hester, W.G., 1983, Ground water in the greater Atlanta region, Georgia: Georgia Geological Survey Information Circular 63, 144 p.

Davis, M.C., and Turlington, K.R., 1987, Ground-water quality and availability in Georgia for 1986: Georgia Geologic Survey Circular 12C, 84 p.

Drever, J.I., 1988, The Geochemistry of Natural Waters (2nd edn.): Englewood Cliffs, N.J., Prentice-Hall, 437 p.

Drever, J.I., and Clow, D.W., 1995, Weathering rates in catchments, in White, A.F., and Brantley, S.L., eds., Chemical weathering rates of silicate minerals: Mineralogical Society of America Reviews in Mineralogy, v. 31, p. 463-483.

Frape, S.K., Blyth, A.R., Jones, M.G., Blomqvist, R., Tullborg, E.-L., McNutt, R.H., McDermott, F., and Ivanovich, M., 1992, A comparison of calcite fracture mineralogy and geochemistry for the Canadian and Fennoscandian Shields, in Kharaka, Y.K., and Maest, A.S., Water-Rock Interaction: Proceedings of the 7th International Symposium on Water-rock Interaction, Vol. 1: Rotterdam, A.A. Balkema, p. 787-791.

Garrels, R.M., 1967, Genesis of some ground waters from igneous rocks, in Abelson, P.H., ed., Researches in Geochemistry, v. 2: New York, John Wiley & Sons, p. 405-420.

Hanor, J.S., 1983, Fifty years of development of thought on the origin and evolution of subsurface sedimentary brines, in Boardman, S.J., ed., Revolution in the Earth Sciences: Dubuque, Kendall/Hunt Publishing Co., p. 99-111.

Hanor, J.S., 1987, Origin and migration of subsurface sedimentary brines: Society of Economic Paleontologists and Mineralogists Short Course 21, 247 p.

Hesse, R., 1988, Origin of chert: diagenesis of biogenic siliceous sediments: Geoscience Canada, v. 15, p. 171-192.

Hodler, T.W., and Schretter, H.A., 1986, The Atlas of Georgia: Athens, Georgia, Institute of Community and Area Development, 273 p.

Huddleston, P.F., and Hetrick, J.H., 1986, Upper Eocene stratigraphy of central and eastern Georgia: Georgia Geological Survey Bulletin 95, 78 p.

Jones, B.F., and Bowser, C.J., 1978, The mineralogy and related chemistry of lake sediments, in Lerman, A., ed., Lakes-Chemistry, Geology, Physics: New York, Springer Verlag, p. 179-235.

Kantor, W., and Schwertmann, U., 1974, Mineralogy and genesis of clays in red-black soil toposequences on basic igneous rocks in Kenya: Journal of Soil Science, v. 25, p. 67-78.

Krause, R.E., and Randolph, R.B., 1989, Hydrology of the Floridan aquifer system in southeast Georgia and adjacent parts of Florida and South Carolina: U.S. Geological Survey Professional Paper 1403-D, 65 p.

Krauskopf, K.B., 1979, Introduction to Geochemistry (2nd edn.): New York, McGraw-Hill, 617 p.

Kron, A, and Stix, J., 1982, Geothermal gradient map of the United States exclusive of Alaska and Hawaii: National Geophysical Data Center.

Kron, A., Wohletz, K., and Tubb, J., 1991, Geothermal gradient contour map of the United States: Los Alamos, New Mexico, Los Alamos National Laboratory, 1:7,630,000.

Kundell, J.E., 1978, Ground Water Resources of Georgia: Athens, Georgia, University of Georgia Institute of Government, 139 p.

Land, L.S., and Macpherson, G.L., 1992, Origin of saline formation waters, Cenozoic section, Gulf of Mexico sedimentary basin: American Association of Petroleum Geologists Bulletin, v. 76, p. 1344-1362.

Land, L.S., and Milliken, K.L., 1981, Feldspar diagenesis in the Frio Formation, Brazoria County, Texas Gulf Coast: Geology, v. 9, p. 314-318.

Lawton, D.E., Marsalis, W.E., and fifteen others, 1976, Geologic Map of Georgia: Georgia Department of Natural Resources, 1:500,000.

Lee, R.W., 1993, Geochemistry of groundwater in the Southeastern Coastal Plain aquifer system in Mississippi, Alabama, Georgia, and South Carolina: U.S. Geological Survey Professional Paper 1410-D, 72 p.

Lee, R.W., and Strickland, D.J., 1988, Geochemistry of groundwater in Tertiary and Cretaceous sediments in eastern Georgia, South Carolina, and southeastern North Carolina: Water Resources Research, v. 24, p. 291-303.

LeGrand, H.E., 1967, Ground Water of the Piedmont and

Blue Ridge provinces in the southeastern states: U.S. Geological Survey Circular 538, 11 p.

Lovley, D.R., and Chapelle, F.H., 1995, Deep subsurface microbial processes: Reviews of Geophysics, v. 33, p. 365-381.

Melear, N.D., 1990, Clay minerals and ferruginous minerals formed during weathering of granitic rocks of the Georgia Piedmont: M.S. Thesis, University of Georgia, 69 p.

Mirecki, J.E., and Parks, W.S., 1994, Leachate geochemistry at a municipal landfill, Memphis, Tennessee: Ground Water, v. 32, p. 390-398.

Piper, A.M., 1953, A graphic procedure in the geochemical interpretation of water analysis: U.S. Geological Survey Ground-Water Note 12, 14 p.

Sonderegger, J.L., Pollard, L.D., and Cressler, C.W., 1978, Quality and availability of ground water in Georgia: Georgia Geological Survey Information Circular 48, 25 p.

Sprinkle, C.L., 1989, Geochemistry of the Floridan aquifer system in Florida and in parts of Georgia, South Carolina, and Alabama: U.S. Geological Survey Professional Paper 1403-I, 105 p.

Steele, W.M., 1987, Ambient ground-water chemistry and quality in the Floridan aquifer system in Georgia: Georgia Geologic Survey Hydrologic Atlas 17.

Stewart, J.W., 1962, Relation of permeability and jointing in crystalline metamorphic rocks near Jonesboro, Georgia: U.S. Geological Survey Professional Paper 450-D, p. D168-170.

Stringfield, V.T., 1966, Artesian water in Tertiary limestone in the southeastern states: U.S. Geological Survey Professional Paper 517, 226 p.

Stumm, W., and Morgan, J.J., 1981, Aquatic Chemistry (Second Edn.): New York, John Wiley and Sons, 780 p.

Turner, J.V., Anderson, T.F., Sandberg, P.A., and Goldstein, S.J., 1986, Isotopic, chemical, and textural relations during the experimental alteration of biogenic high-magnesium calcite: Geochimica et Cosmochimica Acta, v. 50, p. 495-506.

Velbel, M.A., 1985, Hydrogeochemical constraints on mass balances in forested watersheds of the southern Appalachians, in Drever, J.I., ed., The Chemistry of Weathering: Dordrecht, D. Reidel Publishing Co., p. 231-247.

Waber, N., and Nordstrom, D.K., 1992, Geochemical modeling of granitic ground waters at the Stripa site (Sweden) using a mass-balance approach, in Kharaka, Y.K., and Maest, A.S., Water-Rock Interaction: Proceedings of the 7th International Symposium on Water-rock Interaction, Vol. 1: Rotterdam, A.A. Balkema, p. 243-246.

Walter, L.M., 1985, Relative reactivity of skeletal carbonates during dissolution: implications for diagenesis, in Schneidermann, N., and Harris, P.M., eds., Carbonate Cements: Society of Economic Paleontologists and Mineralogists Special Publication 36, p. 3-16.

Wanty, R.B., Folger, P.F., Frishman, D., Briggs, P.H., Day, W.C., and Poeter, E., 1992, Weathering of Pikes Peak Granite: Field, experimental, and modelling observations, in Kharaka, Y.K., and Maest, A.S., Water-Rock Interaction: Proceedings of the 7th International Symposium on Water-rock Interaction, Vol. 1: Rotterdam, A.A. Balkema, p. 599-602.

White, A.F., and Brantley, S.L., 1995, Chemical weathering rates of silicate minerals: an overview, in White, A.F., and Brantley, S.L., eds., Chemical weathering rates of silicate minerals: Mineralogical Society of America Reviews in Mineralogy, v. 31, p. 1-22.

White, W.B., 1988, Geomorphology and Hydrology of Karst Terrains: Oxford, Oxford University Press, 464 p.

Williams, H., 1978, Tectonic lithofacies map of the Appalachian orogen: Memorial University of Newfoundland Map Number 1, 1:1,000,000.

Williams, L.A., and Crerar, D.A., 1985, Silica diagenesis, II: General mechanisms: Journal of Sedimentary Petrology, v. 55, p. 312-321.

APPENDIX 1: SOURCES OF DATA

Clarke, J.S., Faye, R.E., and Brooks, R., 1983, Hydrogeology of the Providence aquifer of southwest Georgia: Georgia Department of Natural Resources Hydrologic Atlas 11.

Clarke, J.S., Faye, R.E., and Brooks, R., 1984, Hydrogeology of the Clayton aquifer of southwest Georgia: Georgia Department of Natural Resources Hydrologic Atlas 13.

Clarke, J.S., Hacke, C.M., and Peck, M.F., 1990, Geology and ground-water resources of the coastal area of Georgia: Georgia Geological Survey Bulletin 113, 106 p.

Cressler, C.W., 1963, Geology and ground-water resources of Catoosa County, Georgia: Georgia Geological Survey Information Circular 28, 19 p.

Cressler, C.W., 1964, Geology and ground-water resources of the Paleozoic rock area, Chattooga County, Georgia: Georgia Geological Survey Information Circular 27, 14 p.

Cressler, C.W., 1964, Geology and ground-water resources of Walker County, Georgia: Georgia Geological Survey Information Circular 29, 15 p.

Cressler, C.W., 1970, Geology and ground-water resources of Floyd and Polk Counties, Georgia: Georgia Geological Survey Information Circular 39, 95 p.

Cressler, C.W., Thurmond, C.J., and Hester, W.G., 1983, Ground water in the greater Atlanta region, Georgia: Georgia Geological Survey Information Circular 63, 144 p.

Cressler, C.W., Blanchard, H.E., Jr., and Hester, W.G., 1979, Geohydrology of Bartow, Cherokee, and Forsyth Counties, Georgia: Georgia Geological Survey Information Circular 50, 45 p.

Croft, M.G., 1964, Geology and ground-water resources of Dade County, Georgia: Georgia Geological Survey Information Circular 26, 17 p.

Grantham, R.G., and Stokes, W.R., 1976, Ground-water quality data for Georgia: U.S. Geological Survey, 216 p.

Hicks, D.W., Krause, R.E., and Clarke, J.S., 1981, Geohydrology of the Albany area, Georgia: Georgia Geological Survey Information Circular 57, 31 p.

Krause, R.E., 1972, Effects of ground-water pumping in parts of Liberty and McIntosh Counties, Georgia, 1966-70: Georgia Geological Survey Information Circular 45, 15 p.

Lee, R.W., 1984, Ground-water quality data from the southeastern coastal plain, Mississippi, Alabama, Georgia, South Carolina, and North Carolina: US Geological Survey Open-File Report 84-237.

Matthews, S.E., and Krause, R.E., 1984, Hydrogeologic data from the U.S. Geological Survey test wells near Waycross, Ware County, Georgia: U.S. Geological Survey Water-Resources Investigations Report 83-4204, 29 p.

McConnell, J.B., Busenberg, E., and Plummer, L.N., 1994, Water-resources data for the Valdosta area, south-central Georgia, 1961-93: U.S. Geological Survey Open-File Report 94-350, 58 p.

Owen, V., Jr., 1963, Geology and ground-water resources of Mitchell County, Georgia: Georgia Geological Survey Information Circular 24, 40 p.

Sever, C.W., 1964, Geology and ground-water resources of crystalline rocks Dawson County, Georgia: Georgia Geological Survey Information Circular 30, 32 p.

Sever, C.W., 1965, Ground-water resources and geology of Seminole, Decatur, and Grady Counties, Georgia: U.S. Geological Survey Water-Supply Paper 1809-Q.

Sever, C.W., 1966, Reconnaissance of the ground water and geology of Thomas County, Georgia: Georgia Geological Survey Information Circular 34, 14 p.

Wait, R.L., 1965, Geology and occurrence of fresh and brackish water in Glynn County, Georgia: U.S. Geological Survey Water-Supply Paper 1613-E.

SOUTHEASTERN GEOLOGY
V. 36, No. 3, November 1997, p. 123-132

TWO HIGH-SILICA GNEISSES FROM THE DADEVILLE COMPLEX OF ALABAMA'S INNER PIEDMONT

MICHAEL J. NEILSON

Department of Geology
The University of Alabama at Birmingham
Birmingham, AL 35294

THOMAS L. SEAL AND STEPHEN A. KISH

Department of Geology
Florida State University
Tallahassee, FL 32306

ABSTRACT

Two high-silica gneisses, the Camp Hill Gneiss (mean SiO_2 = 74.3%) and the Chattasofka Creek Gneiss (mean SiO_2 = 74.8%), occur as small rootless plutons in the Dadeville Complex of Alabama. The Camp Hill Gneiss is of tonalitic composition, geochemically is a low-Al_2O_3 trondhjemite-tonalite and probably formed in a volcanic arc setting. The Chattasofka Creek Gneiss is granitic in composition, highly peraluminous and probably formed in a collisional setting.

INTRODUCTION

In his summary of the ages of southern Appalachian plutons, Sinha (1988) described those from the Dadeville Complex of Alabama as "undefined." Such a description could well be applied to all aspects of felsic plutonism in the Dadeville Complex of Alabama. No felsic rocks have been dated by techniques other than K-Ar, and only recently have individual bodies been mapped. Originally called the Sougahatchee granite by Adams (1933), these bodies have been shown to be gneissic and have compositions that vary from granitic to tonalitic. (See Steltenpohl and others, 1990 for a summary of previous work.) As granitic rocks can shed light on the tectonic settings of the terranes in which they occur and may be used to correlate neighboring terranes in an orogen, detailed field, petrographic, geochemical and geochronological studies are essential for understanding the evolution of the orogen. As a contribution to the understanding of the evolution of the Southern Appalachians, this paper presents new geochemical data on the felsic gneisses of the Dadeville Complex of Alabama, defines their petrographic and geochemical characteristics, and determines their tectonic settings.

GEOLOGY OF THE DADEVILLE COMPLEX

The Dadeville Complex is a part of the Inner Piedmont, a composite terrane that occurs between the Coastal Plain onlap in Alabama and the Sauratown Mountains window and the Smith River allochthon in Virginia and western North Carolina. In Alabama and western Georgia, the Inner Piedmont consists of the Dadeville Complex, located in the northwestern portion of the terrane and dominated by metaigneous rocks, and the Opelika Complex, composed predominantly of metasedimentary rocks. The Dadeville and Opelika complexes are separated by the Stonewall line, a discontinuity of unknown origin (Adams, 1926, 1933; Bentley and Neathery, 1970). Detailed mapping of the Dadeville Complex in Alabama is restricted to the area surrounding Dadeville in Tallapoosa County (Figure 1).

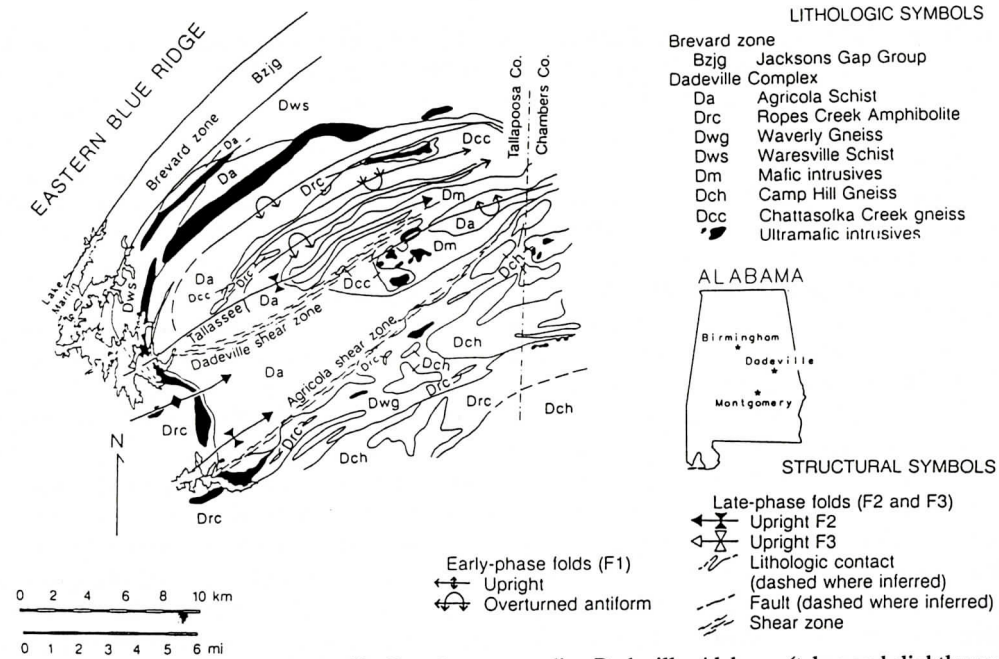

Figure 1. Geologic map of the Dadeville Complex surrounding Dadeville, Alabama (taken and slightly modified from Steltenpohl and others, 1990, Plate 1).

Lithologic Units

In addition to the felsic gneisses, five lithologic units are recognized in the Dadeville Complex near Dadeville (Steltenpohl and others, 1990): Ropes Creek Amphibolite, Waresville Schist, Waverly Gneiss, Agricola Schist, and mafic and utramafic intrusives.

The Ropes Creek Amphibolite (Bentley and Neathery, 1970) is the most common unit in the Dadeville Complex and consists mainly of well-foliated amphibolite with minor interlayed slightly-foliated felsic layers (Stow and others, 1984). Small volumes of quartzite and sillimanite-bearing schist also occur. The amphibolites have tholeiitic basaltic compositions and are characterized by moderate TiO_2 and alkali contents, moderate iron enrichment relative to magnesia, and flat REE patterns with slight LREE enrichment. These rocks have an E-MORB signature, and their progenitors were probably generated by partial melting of an undepleted mantle beneath a back-arc basin (Stow and others, 1984). The felsic layers are dacitic to rhyolitic in composition, and are characterized by large positive Eu anomalies and slight LREE and MREE depletion. The felsic layers are interpreted as either felsic volcanics emplaced in a back-arc basin or the result of metamorphic differentiation of the amphibolite progenitors (Hall and Salpas, 1990).

The Waverly Gneiss consists of leucocratic feldspathic and hornblende gneiss with minor amphibolite, calc-silicate rock, muscovite schist, and quartzite (Raymond and others, 1988). The Waverly is distinguished from the Ropes Creek by its light-colored saprolite, the result of the predominance of feldspathic and hornblende gneisses (T. L. Neathery, personal communication).

The Waresville Schist, which occurs in contact with the Brevard Zone, consists of chlorite-actinolite schist, metaquartzite and amphibolite. On the basis of chemical similarities, Stow and others (1984) consider the Waresville to be altered and retrograded Ropes Creek Amphibolite.

The Agricola Schist (Sears and others, 1981) consists of approximately equal amounts of interlayered gneiss and schist. Common

lithologies include garnetiferous-muscovite biotite schist and paragneiss, which are occasionally kyanite- or silliminite-rich. Minor amphibolite, hornblende gneiss, and quartzite occur in this unit.

Mafic and ultramafic intrusive rocks occur in complexes (shown as Mafic intrusives and Ultramafic intrusives on Figure 1) that contain metagabbro, metanorite, metaorthopyroxenite, massive amphibolite, actinolite schist and Ropes Creek Amphibolite. Where mapped in detail, the complexes consist of sills, layered intrusions, and dikes that intrude the Ropes Creek Amphibolite. The intrusive rocks are divided into two suites, the Doss Mountain and Slaughters suites (Neilson and Stow, 1986). The Doss Mountain suite consists of metaorthopyroxenite and metanorite and their more altered equivalents, actinolite schist and massive, coarse-grained amphibolite; whereas the Slaughters suite consists of metagabbro. The Doss Mountain rocks have low concentrations of alkalis, REE, TiO_2, and incompatible elements; whereas the Slaughters rocks are rich in incompatible elements, have moderate alkali contents and higher REE and TiO_2 contents. The Doss Mountain rocks are tholeiitic and probably formed in an arc environment by partial melting of a depleted source. The Slaughters rocks are calc-alkaline and also indicate an arc tectonic setting (Neilson and Stow, 1986).

Deformational History

As described by Steltenpohl and others (1990), the earliest recognized deformational event (D_1) in the Dadeville Complex overlapped with the amphibolite facies dynamothermal metamorphism (M_1) that formed kyanite and sillimanite in metapelitic units. D_1-M_1 formed the main schistosity (S_1) and tight to isoclinal similar folds (F_1) that plunge gently to the northeast and southwest. During late-D_1 high-temperature ductile deformation zones developed that were later reactivated during or near the end of D_2 when more brittle shearing occurred, forming the Dadeville and Agricola shear zones (Figure 1). Based on a 369 ±5 Ma date on the syn-D_1 Farmville Metagranite (Goldberg and Burnell, 1987) from the Opelika Complex, which has an identical deformational history to that of the Dadeville Complex beginning with prograde regional metamorphism (Steltenpohl and others, 1990), D_1 probably was an Acadian event. All units in the Dadeville Complex, including the felsic gneisses were affected by the D_1-M_1 event.

A later deformation appears to have been a protracted event that generated D_2 and D_3 structures and was broadly coincident with a greenschist-facies retrogressive metamorphism (M_2). D_2 structures include spaced and crenulation cleavages (S_2), and recumbent to inclined, broad to tight folds in schists to inclined to upright, tight to rather broad, chevron and kink-like folds (F_2). The dominant D_3 structures are shallow, northwest-plunging cross folds (F_3) that range from broad, gently plunging warps to tight, often straight-limbed, chevron- and kink-like styles. The age of the late-phase deformations is loosely bracketed between the Devonian and Mesozoic because D_2 structures clearly overprint fabrics and structures formed during the late Devonian metamorphic peak, and aeromagnetic evidence indicates that Late Triassic to Early Jurassic diabase dikes crosscut D_2 structures (Bentley and Neathery, 1970; Osborne and others, 1988). Based on a 296 ±4 Ma Rb-Sr mineral isochron for a sample of tectonized Farmville Metagranite, Goldberg and Steltenpohl (1988) suggested an Alleghanian age for D_2.

FIELD RELATIONS AND PETROGRAPHY OF THE FELSIC GNEISSES

About 40 percent of the Dadeville Complex is underlain by medium- to coarse-grained, poorly-foliated felsic gneisses that display granoblastic, gneissic and mortar textures. Some leucocratic specimens contain only a weakly-developed mineral lineation defined by aligned biotite. Although Bentley and Neathery (1970) mapped these felsic rocks as a single unit

(Granite gneiss - undifferentiated), they described two variants: the Rock Mills granite and the Camp Hill granite. The Rock Mills granite occurs in the northeastern part of the Dadeville Complex and consists of either a coarse-grained, slightly foliated leucocratic granitic gneiss or a well-foliated biotite-granite gneiss. The Camp Hill granite occurs in the southwestern part of the Complex and consists of foliated granitic to quartz monzonitic gneisses. In the vicinity of Dadeville, Neilson (1987) divided Bentley and Neathery's (1970) Camp Hill granite into two mappable units: the tonalitic Camp Hill Gneiss (CHG) and the granitic Chattasofka Creek Gneiss (CCG). The distribution of the CHG and CCG near Dadeville is shown on Figure 1.

The CHG and CCG have several features in common. Both appear to be rootless plutons showing concordant contacts with the surrounding units. Individual plutons of both units have been folded by F_1 isoclinal folds (Figure 1). Amphibolitic and schistose xenoliths occur within both gneisses. Based on their petrography, the xenoliths are interpreted as pieces of the Ropes Creek Amphibolite and Agricola Schist, respectively, and, thus, both felsic units are considered to post-date sedimentation and volcanism in the Dadeville Complex (Neilson, 1987).

Cross-cutting relationships between the CHG and CCG are nowhere found in the area mapped, but evidence from the composition of micas in the gneisses suggests that the CHG might be older than the CCG. Drummond and Neilson (in preparation) show that biotite and muscovite compositions from the CCG are typical of igneous micas, whereas the micas from the CHG have typical metamorphic compositions. They further suggest that the CHG protolith formed pre D_1-M_1 and that the CCG formed late in the same event. Alternatively, the igneous micas in the CCG may be relict, the result of limited metamorphic fluid movement within the CCG.

The CHG occurs as several plutons that are usually surrounded by either Waverly Gneiss or Ropes Creek Amphibolite (see Figure 1). The gneiss is medium- to coarse-grained, poorly-foliated, light gray in color when fresh, and characterized by the very low abundance of microcline (average 2.5%: Neilson, 1987). The major ferromagnesian mineral is moderate brown biotite that is occasionally accompanied by dark yellow green hornblende. Both primary and secondary muscovite are present. Plagioclase is typically unzoned and contains quartz and epidote inclusions. Accessory minerals include opaque oxides, sphene, skeletal and prismatic epidote, and rare zircon and garnet.

The CCG occurs as a hairpin-shaped pluton just to the north of Dadeville, where its southeastern boundary is truncated by the Dadeville shear zone (see Figure 1). It is distinguished from the CHG by the presence of abundant microcline (average 30%: Neilson, 1987) and primary muscovite. The alkali feldspar is microcline microperthite, the plagioclase is occasionally zoned, and myrmekite is common. Accessory minerals include epidote, sphene, apatite, garnet and opaque oxides. Some specimens close to the shear zones show a mortar texture with large clasts of both feldspars set in a matrix of feldspar, quartz and dusky brown biotite.

GEOCHEMISTRY OF THE FELSIC GNEISSES

Tables 1 and 2 present major and trace element data for the CHG and CCG. Silicon was determined by spectrophotometry using the procedure described by Shapiro (1974); Al, Fe, Mg, Na, and K were analyzed by standard atomic absorption techniques using calibrated solutions prepared from rock standards; Ca, Mn, Ti, P, Rb, Sr and Zr were determined by X-ray fluorescence (Rh target) on fused glass discs (Norrish and Hutton, 1969); and U and Th data were obtained by gamma-ray spectrometry using a technique modified from Adams and Gasparina (1970). Estimated analytical uncertainties (precision) for major elements are less than 2%, except for P and Mn. Estimated analytical uncertainties for trace elements by XRF

Table 1. Major Oxide Analyses (weight percent) of the Chattasofka Creek and Camp Hill Gneisses.

	SiO_2	TiO_2	Al_2O_3	Fe_2O_{3T}	MnO	MgO	CaO	Na_2O	K_2O	P_2O_5	LOI
Chatasofka Creek Gneiss											
X-25	75.7	0.1	13.6	1.0	0.01	0.1	0.5	2.1	5.6	0.0	1.6
X-26	76.1	0.2	13.8	1.0	0.02	0.1	0.7	2.1	5.4	0.1	1.9
X-30	75.0	0.3	14.3	1.4	0.04	0.6	0.9	1.9	5.4	0.1	1.7
X-32	73.3	0.2	15.0	1.3	0.04	0.2	0.6	2.0	5.9	0.2	2.1
X-35	76.5	0.1	13.4	0.9	0.01	0.1	0.2	1.5	6.0	0.0	2.1
X-37	74.7	0.3	14.5	1.9	0.04	0.7	1.0	2.7	4.1	0.1	2.1
X-39	71.0	0.3	15.4	2.4	0.04	0.9	1.1	1.6	4.3	0.1	3.0
H-9	75.4	0.2	13.0	1.2	0.03	0.1	0.7	2.4	4.9	0.0	1.7
H-23	75.2	0.0	15.3	0.5	0.03	0.1	0.4	1.9	5.9	0.0	2.2
CN-176	75.6	0.1	14.4	0.7	0.05	0.1	1.0	2.3	5.2	0.1	1.8
CHG-27	74.0	0.2	14.7	1.9	0.04	0.1	0.6	2.4	4.7	0.0	2.3
Mean	74.8	0.2	14.3	1.3	0.03	0.3	0.7	2.1	5.2	0.1	2.0
Camp Hill Gneiss											
CHG-2	73.2	0.3	13.8	4.1	0.09	1.4	3.2	3.5	1.2	0.1	0.6
CHG-3	73.8	0.2	14.0	2.9	0.06	0.6	2.5	4.0	1.0	0.0	0.8
CHG-13	75.9	0.3	13.5	2.5	0.10	0.3	2.2	4.2	1.0	0.2	0.7
CHG-14	75.0	0.4	13.8	3.2	0.16	0.9	2.0	4.0	1.2	0.1	1.0
CHG-17	75.0	0.3	12.8	2.8	0.07	0.7	2.5	3.9	1.2	0.1	0.5
CHG-18	77.4	0.2	11.5	1.8	0.01	0.9	2.8	3.6	0.6	0.0	0.6
CHG-20	72.8	0.3	13.7	2.7	0.07	0.8	2.5	3.3	1.5	0.0	1.8
CHG-21	74.8	0.2	13.8	2.4	0.05	0.7	2.1	4.6	0.9	0.0	0.6
CHG-29	74.1	0.3	14.2	3.2	0.09	0.7	3.0	4.1	0.9	0.1	0.4
CHG-34	73.5	0.3	14.1	2.0	0.08	0.6	1.7	4.6	1.3	0.1	0.8
87-CH-1	74.1	0.3	13.0	3.9	0.09	1.1	3.2	3.6	1.1	0.0	0.3
87-CH-3	72.5	0.2	14.4	4.2	0.11	1.3	3.6	3.4	0.8	0.0	0.7
Mean	74.3	0.3	13.5	3.0	0.08	0.8	2.6	3.9	1.0	0.1	0.7

are typically less than 10%. REE, Hf and Ta were obtained by neutron activation analysis and Nb and Y were obtained by XRF methods. Analytical uncertainties for these elements are less than 10%. However, the concentrations of Ta were near detection limits, and uncertainties may be higher.

Both gneisses are silica-rich (mean SiO_2 = 74.3% and 74.8%, respectively, for the CHG and CCG), resulting in mean normative quartz in excess of 40% for each. Variations in major elements for each gneiss can be described by their correlation with SiO_2. In the CCG, most oxides show moderate to strong negative correlation with silica (ranging from r = -0.50 for SiO_2 - CaO to -0.77 for SiO_2 - Fe_2O_{3t}). Na_2O and K_2O are the exceptions, both of which show weak to moderate positive correlation (r = +0.16 and +0.50, respectively). In the CHG most oxides show weak negative correlation with silica, with only Al_2O_3 showing strong negative correlation (r = -0.78). The moderate negative correlation of K_2O with silica (r = -0.50) is notable in the CHG, a trend that is uncommon in most felsic bodies.

Both the CCG and the CHG are peraluminous, with mean molar Al_2O_3/(molar CaO + Na_2O + K_2O) being 1.4 and 1.1, respectively. Both units are also moderately, but not strongly, enriched in iron relative to magnesia (mean FeO/[FeO + MgO] = 0.80 and 0.76, respectively).

Although large difference in the mean Rb concentrations exist, the mean K/Rb of each rock is indistinguishable: 258 in the CCG and 248 in the CHG, and similar to the continental crustal average (Taylor and McLennan, 1985). Within the CHG, both Ba and Rb show moderate and strong positive correlation with K_2O (r = +0.63 and 0.89, respectively), whereas Ba and Rb show moderate negative and positive correlation with K_2O (r = -0.59 and +0.63, respectively).

The CHG contains higher REE concentrations than does the CCG. As shown by the chondrite normalized patterns in Figure 2, the major difference being in the higher concentrations of HREE in the CHG. The patterns of the

Table 2. Trace Element Analyses (parts per million) of the Chattasofka Creek and Camp Hill Gneisses.

	Rb	Sr	Ba	U	Th	Ta	Nb	Ce	Hf	Zr	Sm	Y	Yb	La	Nd	Eu	Tb	Lu
Chattasofka Creek Gneiss																		
X-25	132	77	279	1.8	13.2		16			127	0.6		0.3	5.1		0.2		
X-26	123	101	408	2.2	11.4	2.2	12	40	4.2	123	0.9		0.5	8.4	5	0.4		0.08
X-30	132	210	778	2.8	35.1		22			165								
X-32	228	63	389	3.6	15.5	3.7		51	3.5	82	5.5		0.4	28.4	26	1.0	0.5	0.05
X-35	191	113	409	2.9	17.9	1.4	4	25	5.1	106	0.4		0.3	2.5		0.3		0.05
X-37	131	107	1466	1.6	19.3		14			166								
X-39	139	76	526	1.7	24.6					139								
H-9	235	22	221	3.3	39.6		22			115		15						
H-23	234	126	460	3.3	23.8	1.6	3	7	3.2	60	0.6		1.2	1.5		0.2		0.2
CN-176	145	99	326	2.2	12.2		16	5		45	0.4		0.6	2.8	5	0.2	0.5	0.1
CHG-27	162	79	1390	3.6	24.3		12			233								
Mean	168	98	605	2.6	21.5					124								
Camp Hill Gneiss																		
CHG-2	46	110	228	1.1	7.1	2.1	11	30	3.5	93	2.9	16	2.7	14.7	16	0.5	0.7	0.4
CHG-3	32	94	251	0.7	7.0		12			120								
CHG-13	24	84	308	0.7	6.3	1.5	16	23	5.7	116	2.7	39	4.7	11.1	12	0.8	0.7	0.73
CHG-14	41	86	366	0.5	7.0					122								
CHG-17	42	77	241	1.7	9.2	1.0		50		108	4.6		2.5	24.9	24	1.0	0.8	0.38
CHG-18	17	132	17	1.5	8.5	2.0	9	9	4.7	117	2.3	41	3.5	3.4	7	0.8	0.7	0.54
CHG-20	54	75	317	0.8	3.9	1.3	3	25	5.2	131	2.0	14	1.9	7.6	10	0.6	0.5	0.26
CHG-21	27	92	304	1.0	5.3					96								
CHG-29	26	113	334	0.4	7.3		12			98		54						
CHG-34	35	112	404	2.1	15.3		2			112		2						
87-CH-1	40	107	228	1.1	4.7		10			89		27						
87-CH-3	31	100	204	0.5	11.2					90								
Mean	35	99	267	1.0	7.7					108								

CHG are relatively homogeneous, characterized by slight LREE enrichment relative to HREE ($[La/Lu]_N$ = 2.7), flat patterns in the HREE, and a negative Eu anomaly. In contrast, the CCG displays irregular patterns in the LREE and moderate but variable LREE enrichment relative to HREE ($[La/Lu]_N$ = 8.5). Drummond and others (in press) propose that the irregular patterns displayed by the CCG may reflect the control of REE-rich accessory minerals, such as apatite or monazite.

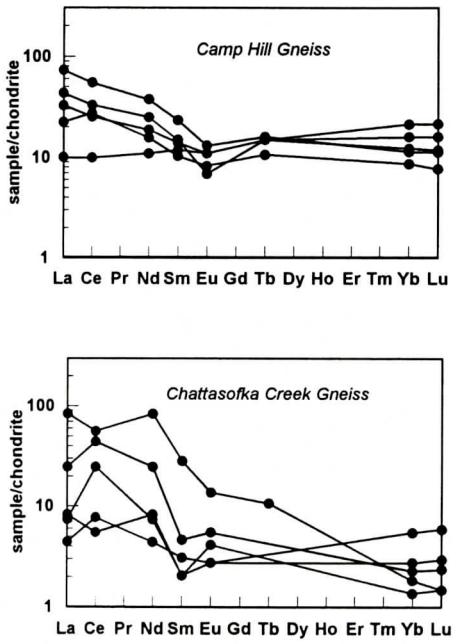

Figure 2. Chondrite-normalized (Wakita and others, 1971) Rare Earth Element (REE) patterns of the Chattasofka Creek and Camp Hill Gneisses.

Using Streckeisen's (1976) classification, Neilson (1987) distinguished the granitic CCG from the tonalitic CHG on the basis of modal mineralogy. The geochemical data support that distinction. On the normative Or:Ab:An diagram of Barker (1979) the CHG plots astride the trondhjemite-tonalite boundary and the CCG plots in the field of granite *sensu stricto* (Figure 3). As Streckesisen's classification does not differentiate between tonalites and trondhjemites and the CHG plots astride the boundary between these rock types, the term tonalitic will be used to describe the CHG's composition.

Two-sample T tests on the major element concentrations of the CCG and CHG show that the rocks are significantly different (at the 95 percentile) in all oxides except SiO_2. Na_2O, K_2O and CaO have the highest absolute T scores, and thus make good discriminators between the two rock types. On a Na-K-Ca weight

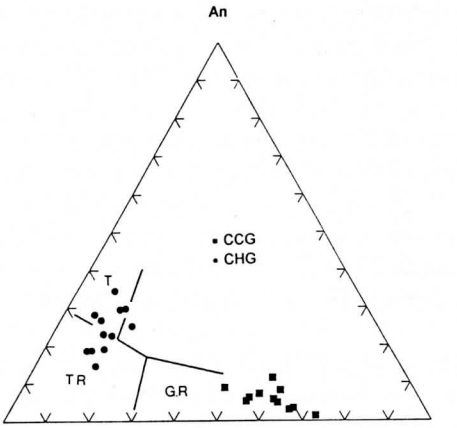

Figure 3. CIPW normative compositions of the Camp Hill Gneiss (filled circles) and the Chattasofka Creek Gneiss (filled squares) in the Ab-Or-An ternary. Classification of rocks from Barker (1979). T: tonalite, TR: trondhjemite, GR: granite.

percent diagram (Figure 4), the fields of the CCG and CHG are clearly delineated, with the CHG plotting close to the calc-alkaline tonalite and the CCG plotting along the extension of the calc-alkaline granite trend of Barker and Arth (1976). The major and trace element concentrations of the CHG match well Barker and Arth's (1976) low-Al_2O_3 trondhjemite-tonalite, which is characterized by less than 15% Al_2O_3 at 70% SiO_2, low Rb and Sr, and REE patterns with a negative Eu anomaly, slight LREE enrichment and flat HREE.

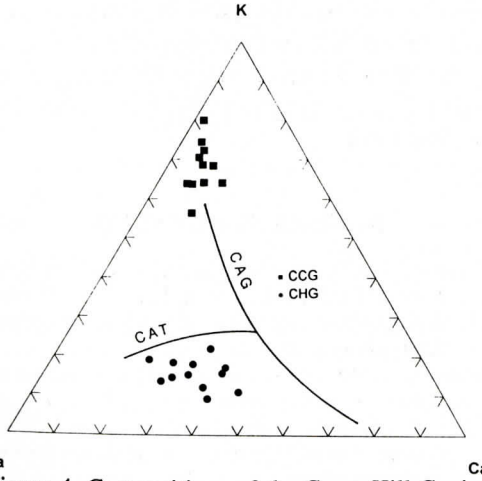

Figure 4. Compositions of the Camp Hill Gneiss (filled circles) and the Chattasofka Creek Gneiss (filled squares) in the Na-Ca-K ternary. Fractionation trends for calc-alkali granite (CAG) and calc-alkali tonalite (CAT) from Barker and Arth (1976).

TECTONIC SETTING

A second objective of this study was to determine the tectonic setting of the CCG and the CHG. Geochemical criteria for distinguishing tectonic settings of felsic plutonic rocks have been developed by Pearce and others (1984),

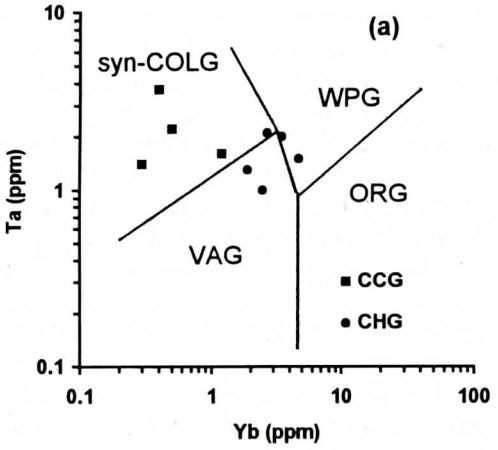

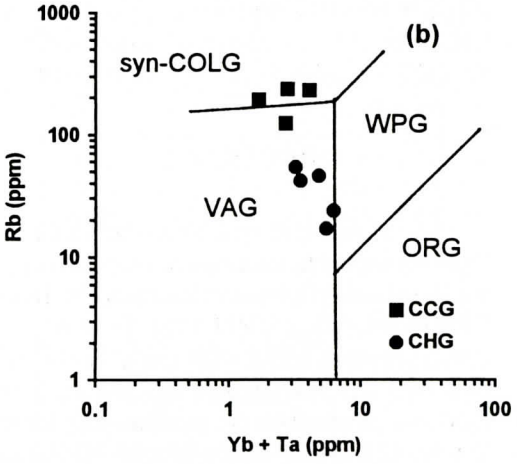

Figure 5. Tectonic discriminant diagrams for the Camp Hill Gneiss (filled circles) and the Chattasofka Creek Gneiss (filled squares). (a) Ta - Yb (b) Rb - Yb + Ta. Boundaries from Pearce and others (1984).

Harris and others (1986), and Maniar and Piccoli (1989), among others. Although terminology differs from scheme to scheme, each recognizes that granites occur in several tectonic settings, such as ocean ridge, volcanic arc, collisional, post-collisional, uplift and within-plate environments.

Trace element patterns for the CCG and CHG when normalized against ocean ridge granite (Pearce and others, 1984) are characterized by depletion of HREE ($Yb_N \leq 0.02$ for the CCG and ≥ 0.035 for the CHG), typical of volcanic arc, syn-collisional and post-collisional granites. The extreme depletion of the HREE in CCG suggests that it may be a syn-collisional granite (or group II of Harris and others, 1986). The highly peraluminous nature of the CCG also suggests a continental collisional setting (Maniar and Piccoli, 1989). On the Ta - Yb diagram, the CCG plots within the syn-collisional granite field (Figure 5a) and astride the syn-collisional/volcanic arc granite field on the Rb - Yb + Ta diagram (Figure 5b). In contrast, the CHG plots at the boundary among the syn-collisonal, volcanic arc and within-plate granite fields on the Yb - Ta diagram (Figure 5a) and in the volcanic arc granite fields of the Rb - Yb + Ta diagram (Figure 5b). The low Rb/Zr ratio of the CHG (mean Rb/Zr = 0.33) is typical of volcanic arc granites (Harris and others, 1986). Thus, the preponderance of evidence suggests that the CHG formed in a volcanic arc setting whereas the CCG formed in a syn-collisional setting.

DISCUSSION

The Camp Hill and Chattasofka Creek Gneisses appear to represent two separate magmatic episodes in the evolution of the Inner Piedmont. The CHG is a low-Al_2O_3 trondhjemite-tonalite with the geochemical characteristics of a volcanic arc "granite." The CCG is a granite with the geochemical characteristics of a syn-collisonal granite. The Camp Hill Gneiss may be part of the extensive subduction-related, late Precambrian to early Ordovician calc-alkaline tonalites and metaluminous granites that are present in several, probably accreted terrains of the Appalachians (Drake and others, 1989; Drummond and others, 1994). Extensive, post-early Ordovician tonalite magmatism has not been reported in the Inner Piedmont (Horton and others, 1991); however, late Silurian to Devonian trondhjemite magmatism is present within the eastern Blue Ridge of the Carolinas (McSween and others, 1991), Georgia, and Alabama.

Peraluminous, potassium-rich granites, similar to the Chattasofka Creek Gneiss are common throughout the Inner Piedmont and appear to span a considerable range in age. The Franklin Gneiss, a batholith-size granitic body in the Inner Piedmont of Georgia approximately 75 km northeast of Dadeville, Alabama, is mineralogically and chemically similar to the CCG and has a Rb-Sr whole rock age of approximately 460 Ma (Seal and Kish, 1990). Within the Inner Piedmont of the Carolinas, other metaluminous granite plutons are present, but they appear to have been emplaced during several, separate periods of magmatism that range from Ordovician to late Devonian (Horton and others, 1991; McSween and others, 1991). As mentioned earlier, the age of the CCG in equivocal: it might have been emplaced following peak metamorphic conditions during the Acadian or it may have an early-to mid-Paleozoic age. Additional geochronological studies of both units will place a critical role in deciphering the igneous history of this portion of the Inner Piedmont.

REFERENCES CITED

Adams, G. I., 1926, The crystalline rocks, *in* Adams, G. I., Butts, C., Stephenson, L. W., and Cooke, C. W., eds., Geology of Alabama: Alabama Geological Survey Special Report 14, p. 25-40.

Adams, G. I., 1933, General geology of the crystallines of Alabama: Journal of Geology, v. 41, p. 159-173.

Adams, J. A. S., and Gasparina, P., 1970, Gamma-ray spectrometry of rocks, Methods in Geochemistry and Geophysics #10: Elsevier, Amsterdam, 295 pp.

Barker, F., 1979, Trondhjemite: definition, environment and hypotheses of origin, *in* Barker, F., ed., Trondhjemites, dacites and related rocks: Elsevier Scientific Publishing Co., Amsterdam, p. 1-12.

Barker, F., and Arth, J. G., 1976, Generation of trondhjemitic-tonalitic liquids and Archean bimodal trondhjemite-basalt suite: Geology, v. 4, p. 596-600.

Bentley, R. D., and Neathery, T. L., 1970, Geology of the Brevard fault zone and related rocks of the Inner Piedmont of Alabama, *in* Bentley, R. D., and Neathery, T. L., eds., Geology of the Brevard fault zone and related rocks of the Inner Piedmont of Alabama: Alabama Geological Society 8th Annual Field Trip Guidebook, p. 1-79.

Drake, A. A., Jr., Sinha, A. K., Laird, J., and Guy, R. E., 1989, The Taconic orogen, *in* Hatcher, R. D., Jr., Thomas, W. A., and Viele, G. W., eds., The Appalachian-Ouachita orogen in the United States: The Geology of North America, v. F-2, Geological Society of American, p. 101-177.

Drummond, M. S., Allison, D. T., and Wesolowski, D. J., 1994, Igneous petrogenesis and tectonic setting of the Elkahatchee quartz diorite, Alabama Appalachians: implications for Penobscotian magmatism in the eastern Blue Ridge: American Journal of Science, v. 294, p. 173-236.

Drummond, M. S. and Neilson, M. J. in prep, Thermobarometry of metamorphic equilibria in the Dadeville Complex, Inner Piedmont, Alabama Appalachians: inverted metamorphic gradient and tectonic implications.

Drummond, M. S., Neilson, M. J., Allison, D. T., and Tull, J. M., in press, Igneous petrogenesis and tectonic setting of granitic rocks from the eastern Blue Ridge and Inner Piedmont, Alabama Appalachians, *in* Sinha, A. K., Whalen, J. B., and Hogan, J. P., eds., The nature of magmatism in the Appalachian orogen. Geological Society of America Memoir.

Goldberg, S. A., and Burnell, J. R., 1987, Rubidium-strontium geochronology of the Farmville granite, Alabama Inner Piedmont, *in* Drummond, M. S., and Green, N. L., eds., Granites of Alabama: Alabama Geological Survey Special Publication, p. 251-257.

Goldberg, S. A., and Steltenpohl, M. G., 1988, Evidence for Alleghanian penetrative deformation in the Inner Piedmont of Alabama: Geological Society of America Abstracts with Programs, v. 20, p. 267.

Hall, G. D., and Salpas, P. A., 1990, Geochemistry of thin-layered amphibolites of the Ropes Creek amphibolite, *in* Steltenpohl, M. G., Kish, S. A., and Neilson, M. J., eds., Geology of the Southern Inner Piedmont, Alabama and southwest Georgia: Southeastern Section Geological Society of America Guidebook for Field Trip VII, p. 79- 89.

Harris, N. B. W., Pearce, J. A., and Tindle, A. G., 1986, Geochemical characteristics of collision-zone magmatism, in Coward, M. P. and Ries, A. C., eds. Collision Tectonics: Geological Society Special Publication 19, p. 67-81.

Horton, J. W., Jr., and McConnell, K. I., 1991, The western Piedmont, *in* Horton, J. W., Jr., and Zullo, V. A. (eds.) The geology of the Carolinas: University of Tennessee Press, Knoxville, p. 36-58.

Maniar, P. D. and Piccoli, P. M. 1989, Tectonic discrimination of granitoids: Geological Society of America Bulletin, v. 101, p. 635-643.

McSween, H. Y., Jr., Speer, J. A., and Fullagar, P. D., 1991, Plutonic rocks, *in* Horton, J. W., Jr., and Zullo, V. A. (eds.) The geology of the Carolinas,: University of Tennessee Press, Knoxville, p. 109-126.

Neilson, M. J., 1987, The felsic gneisses of the Inner Piedmont, *in* Drummond, M. S. and Green, N. L. eds., Granites of Alabama: Granites of Alabama: Alabama Geological Survey Special Publication, p. 9-16.

Neilson, M. J., and Stow, S. H., 1986. Geology and geochemistry of the mafic and ultramafic intrusive rocks, Dadeville belt, Alabama: Geological Society of America Bulletin, v. 97, p. 296-304.

Norrish, K. and Hutton, J. T., 1969, An accurate x-ray spectrographic method for the analysis of a wide range of geologic materials: Geochemica et Cosmochemica Acta, v. 33, p. 431-453.

Osborne, W. E., Szabo, M. W., Neathery, T. L., and Copeland, C. W. Jr., 1988, Geologic map of Alabama: Alabama Geological Survey Special Map 220.

Pearce, J. A., Harris, N. B. W., and Tindle, A. G., 1984, Trace element discrimination diagrams for the tectonic interpretation of granites: Journal of Petrology, v. 25, p. 956-983.

Raymond, D. E., Osborne, W. E., Copeland, C. W., and Neathery, T. L., 1988, Alabama stratigraphy: Alabama Geological Survey Circular 140, 97 p.

Seal, T. W., and Kish, S. A., 1990, The geology of the Dadeville complex of the western Georgian and eastern Alabama inner Piedmont: initial petrographic, geochemical, and geochronological results, *in* Geology of the Southern Inner Piedmont, Alabama and southwest Georgia, Steltenpohl, M. G., Kish, S. A., and Neilson, M. J., eds.: Geological Society of America, Southeastern Section, 39th Annual Meeting, Guidebook for Field Trip VII p. 65-77.

Sears, J. W., Cook, R. B., and Brown, D. E., 1981, Tectonic evolution of the western part of the Pine Mountain window and adjacent Inner Piedmont province, *in* Sears, J. W., ed., Contrasts in tectonic style between the Inner Piedmont terrane and the Pine Mountain window: Alabama Geological Society 18th Annual Field Trip Guidebook, p. 1-13.

Shapiro, L., 1974, Spectrophotometric determination of silica at high concentrations using fluoride as a depolymerizer: Journal of Research of the United States Geological Survey, v. 2, p. 357-360.

Sinha, A. K., 1988, Plutonism in the U. S. Appalachians: American Journal of Science, v. 288-a, p. ix-xii.

Steltenpohl, M. S., Neilson, M. J., Bittner, E. I., Colberg, M. R., and Cook, R. B., 1990, Geology of the Alabama Inner Piedmont terrane: Alabama Geological Survey Bulletin 139, 80 pp.

Stow, S. H., Neilson, M. J., and Neathery, T. L., 1984, Petrography, geochemistry, and tectonic significance

of the amphibolites of the Alabama Piedmont: American Journal of Science, v. 284, p. 416-436.

Streckeisen, A., 1976, To each plutonic rock its proper name: Earth Science Reviews, v. 12, p. 1-33.

Taylor, S R., and McLennan, S. M., 1985, The continental crust: its composition and evolution. Blackwell Publishing Co. Oxford, England, 312 pp.

Wakita, H., Rey, P., and Schmitt, R. A., 1971, Abundances of 14 rare-earth elements and 12 other trace elements in Apollo 12 samples: Proceedings of the 2nd Lunar Science Conference, p. 1319-1329.

SOUTHEASTERN GEOLOGY
V. 36, No. 3, November 1996, p. 133-152

GEOLOGY OF THE ASHE METAMORPHIC SUITE IN THE BEAUCATCHER MOUNTAIN ROAD CUT, ASHEVILLE, NORTH CAROLINA

J. WILLIAM MILLER, JR.

Environmental Studies Program
University of North Carolina at Asheville
Asheville, NC 28804-3299

KAREN H. FRYER

Department of Geology and Geography
Ohio Wesleyan University
Delaware, OH 43015-2398

ABSTRACT

The Ashe Metamorphic Suite (AMS) is exposed spectacularly in the Beaucatcher Mountain road cut, along I-240 in Asheville, North Carolina. The dominant rock type is a gneiss, with weak to strong foliation primarily defined by micas. Subordinate rock types include amphibolite, schist, granofels, and a pegmatitic rock. Whole rock compositions indicate a graywacke protolith for the gneiss, and basalt and/or gabbro protoliths for the amphibolites, garnet granofels, and actinolite schist. The mineral assemblages, which include sillimanite and muscovite, are indicative of upper amphibolite facies metamorphism for the AMS at this location. Foliation is predominantly moderately to steeply northwest-dipping and defines part of a northeast trending subhorizontal fold of the AMS across the quadrangle. Abundant mesoscale folds exhibit intrafolial isoclinal, tight asymmetrical, chevron, sheath and superposed geometries. Gneiss within a near-vertical shear zone is completely annealed. Textures of mylonite series gneisses and schists are partially annealed and retain S-C fabric relations and sigmoidal porphyroclasts. Despite significant tectonism, tabular extensive metamafic units with planar contacts likely represent original layering.

INTRODUCTION

The Beaucatcher Mountain road cut (hereafter referred to as the Beaucatcher cut) was completed in the late 1970's along Interstate 240 in Asheville, North Carolina. It is the largest excavation of its kind in the state (Glass, pers. com., 1993). The cut is about 85 m high and 425 m long, with approximately 400 m of contiguous outcrop (Figures 1, 2) across the trend of the Ashe Metamorphic Suite (AMS). The large area and fresh exposure make the Beaucatcher cut an ideal site for detailed study of the AMS in this region. The purpose of this paper is to describe the character of the metamorphism and structure of the AMS at the Beaucatcher cut. In doing so, we hope to provide additional insight into the history of the AMS and to provide information useful for others who will visit this unique site.

REGIONAL GEOLOGY AND PREVIOUS WORK

Rocks of the AMS have not been studied in detail from the Asheville area previously but have been described from other locations to the north (Rankin, 1970; Butler, 1973; Abbott and Raymond, 1984), including the type locality in Ashe County, North Carolina (Rankin, 1970). In a summary work, Rankin and others (1973) described the AMS as "fine-grained, thinly lay-

Figure 1. Picture of cut, view from SW side of cut looking ENE. The foliation is dominantly moderately to steeply northwest dipping.

ered sulfidic biotite-muscovite gneiss interlayered with varying amounts of mica schist and amphibolite." Other studies of the AMS focused on the mafic rocks of the southern Appalachians (Misra and McSween, 1984), the metamorphic history of the AMS in an area northeast of Boone, North Carolina (Abbott and Raymond, 1984), and the relationship of the AMS to the Gossan Lead massive sulfide deposits (Gair and Slack, 1984). Rankin and others (1973) used texture and lithology, and Abbott and Raymond (1984) used bulk composition and petrotectonic assemblages to conclude that the mica gneisses and schists represent metasedimentary rocks, and that the amphibolites, including hornblende gneisses, represent metabasalts and possibly some metagabbro. Gair and Slack (1984) and Merschat and Wiener (1990) subsequently agreed with these assertions and added that the mica gneiss may also include meta-arkose and felsic pyroclastic rocks, respectively. Misra and Conte (1991) concluded that the amphibolites represent tholeiitic basalts, on the basis of geochemistry. Rankin and others (1993) separated the ultramafic rock-bearing part of the AMS from a northern, ultramafic rock-free unit renamed the Wills Ridge Formation. The Beaucatcher cut lies within the ultramafic rock-bearing AMS *(sensu stricto)*.

The structural character and tectonic history of the AMS is highly controversial. Rankin (1970, 1975) suggested the AMS formed originally as sedimentary and volcanic rocks in a tectonic rift along a continental margin. Wehr and Glover (1985) supported that view and asserted that the "interbedded metagraywacke and graphitic schist with intercalated amphibolite" of the AMS and the Lynchburg Group formed in an extensive deep-water environment. Swanson and Raymond (1977), Abbott and Raymond (1984), Raymond and others (1989), and Willard and Adams (1994) considered the AMS to be, at least in part, a tectonic melange.

ROCK TYPES IN THE BEAUCATCHER CUT

Felsic and lesser amounts of mafic rocks of the Ashe Metamorphic Suite are exposed throughout the Asheville 7.5 minute topographic quadrangle. Ultramafic rocks do not occur in

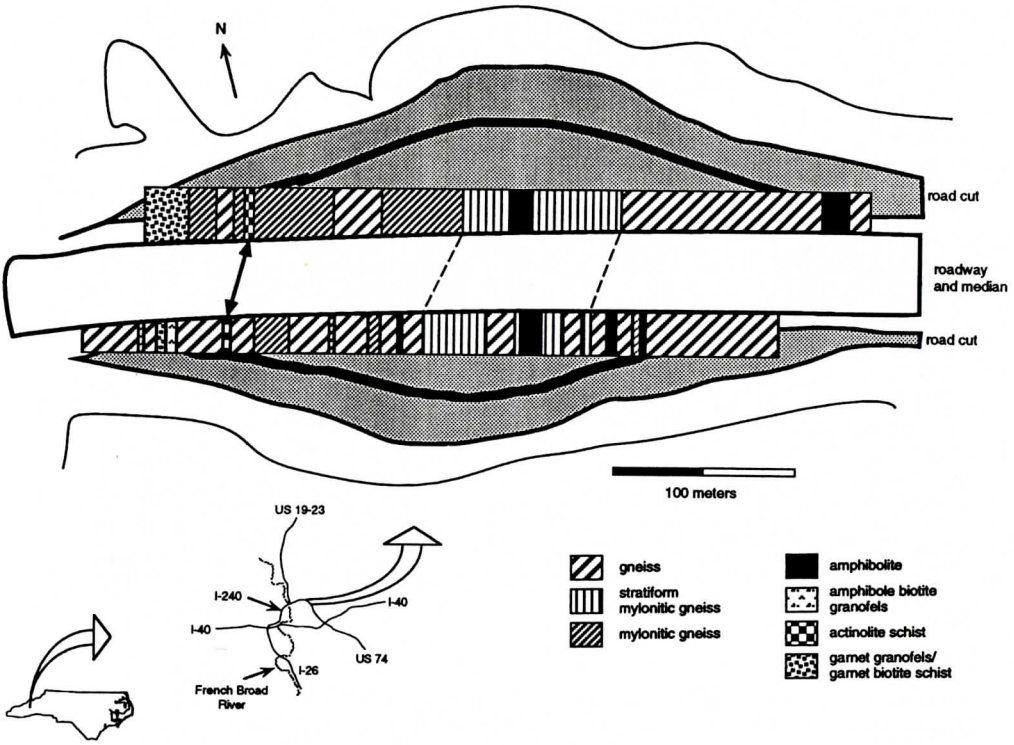

Figure 2. Location and distribution of major rock types in the Beaucatcher cut. Arrow indicates location of actinolite schist and its trend; dashed lines connect the outlines of the stratiform mylonitic gneiss. The actual rock cut is shaded; the thick line approximately parallel to the top of the cut represents a bench.

the Beaucatcher cut but are found elsewhere (Misra and Keller, 1978; Abbott and Raymond, 1984; Raymond and others, 1989; Raymond, 1995, ch. 31).

The most common rock type found in the Beaucatcher cut is referred to in this paper as a gneiss. Other authors have referred to it elsewhere as metagraywacke (Rankin and others, 1973), quartz-feldspar-muscovite schist, mica-quartz-feldspar semischist, quartz-feldspar gneiss (Abbott and Raymond, 1984), and quartz-feldspar granofels (Gair and Slack, 1984). Lesser amounts of amphibolite, schist, and granofels also occur in the cut.

The common gneiss in the Beaucatcher cut is bluish-gray with a consistent mica-defined foliation (Figure 3). The gneissosity in this rock varies from weak mineral banding to almost completely segregated bands of micas versus feldspars and quartz. The texture of the gneiss appears to be similar throughout most of the Asheville 7.5 minute quadrangle, but several variations can be discerned in the relatively fresh exposure of the Beaucatcher cut.

The gneiss (Gn) of the Beaucatcher cut, most common throughout the Asheville quadrangle, is schistose but shows irregular and in many places faint compositional banding. Layers of feldspar and quartz in varying thicknesses (millimeters to centimeters) pass through the gneiss. These feldspathic layers generally parallel the foliation. The minerals of the gneiss are dominantly plagioclase (oligoclase) and quartz, with less but persistent biotite (Tables 1, 2). In many samples, almandine garnet (≥ 2 cm; Table 3) is partly altered to chlorite. Chlorite and muscovite occur in minor amounts, and zircon, apatite, and calcite occur in trace amounts.

Several structurally significant variations of the gneiss occur, based on relative amounts of annealing, development of polycrystalline aggregates, and strength of foliation. These

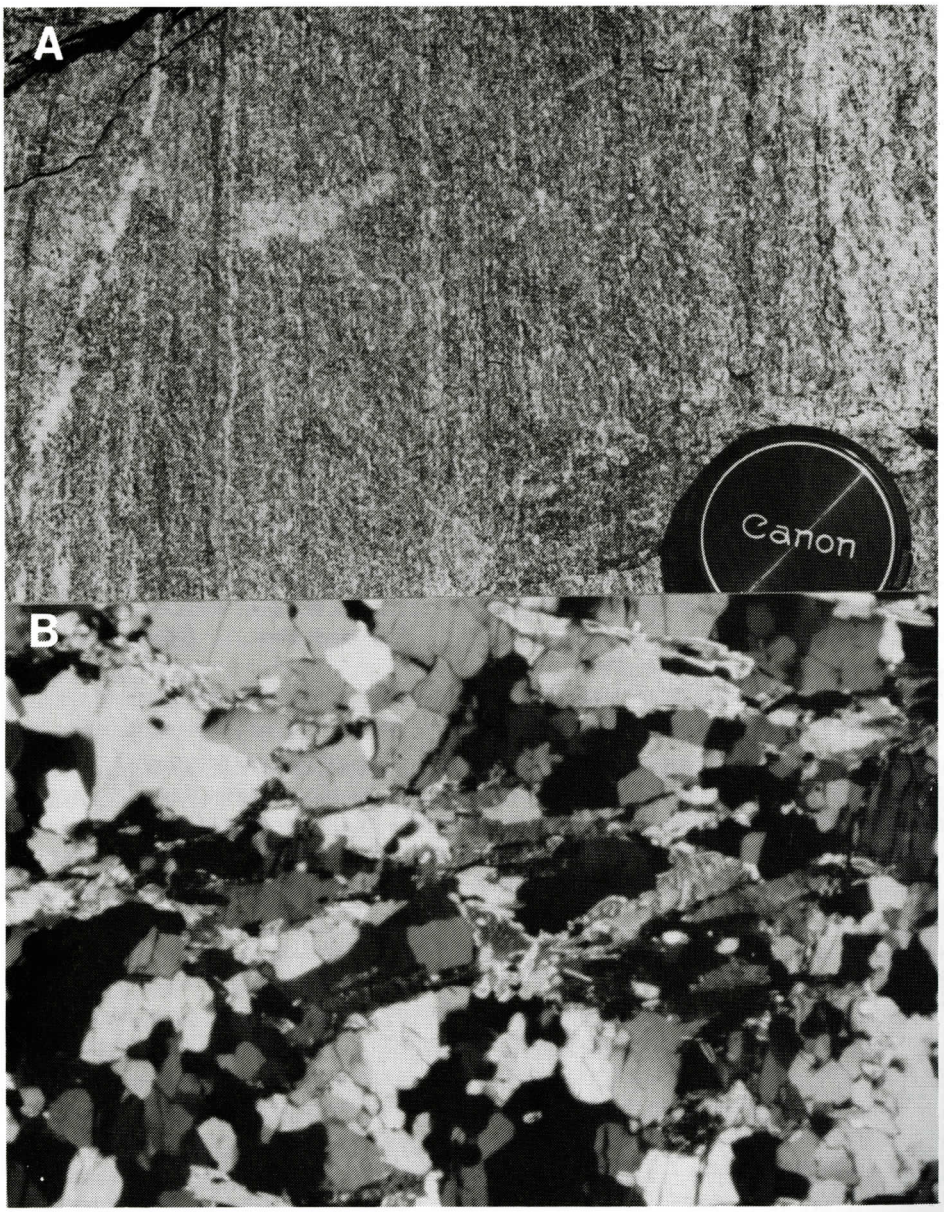

Figure 3. Common gneiss in (a) hand specimen and (b) micrograph. Note the weak foliation. Lens cap in (a) is 6 cm in diameter; long dimension of micrograph is 1.1 mm.

variations are named according to the grain size of the matrix and relative proportion of porphyroclasts and matrix (Twiss and Moores, 1992). The matrix in mylonitic gneiss (MyGn) is > 0.05 mm, whereas the matrix in protomylonite (Pmy) and mylonite (My) is < 0.05 mm. Protomylonite contains approximately 50% porphyroclasts and mylonite approximately 20% porphyroclasts, by volume.

The modifier "stratiform" was added to another variant, the stratiform mylonitic gneiss (SMyGn), to distinguish it from the common gneiss (Gn). The stratiform mylonitic gneiss displays light and dark (Figure 4) contiguous

Table 1. Modes for Beaucatcher Rock Types.*

mineral	Gn B1g	MSch A102-1	Am B8b	ABGf B10	GGf B2	GBSch B12	ActSch ChlAct
plagioclase	43	9	36	79	35	16	10
K-feldspar	•	7	•	•	•	1	tr
quartz	21	8	•	•	•	8	13
garnet	2	•	t	•	49	36	•
biotite	23	21	7	7	5	23	7
muscovite	2	50	•	•	1	6	•
chlorite	7	•	t	3	2	•	•
clinozoisite	•	t	•	•	•	•	•
kyanite	•	5	•	•	3	3	t
sillimanite	t	•	•	•	3	6	•
actinolite	•	•	•	•	•	•	69
hornblende	•	•	54	6	•	•	•
cummingtonite	•	•	•	5	•	•	t
titanite	•	•	•	•	•	t	•
zircon	t	t	•	•	t	t	•
apatite	t	t	t	t	t	•	t
calcite	•	•	•	t	•	t	t
pyrrhotite	t	•	1	t	2	t	•
pyrite	•	•	•	•	•	•	t
chalcopyrite	t	•	t	t	t	t	•
pentlandite	•	•	t	t	t	t	t
rutile	•	•	t	•	t	1	•
ilmenite	2	t	2	t	t	t	•
magnetite	•	t	t	•	•	•	•
hematite	•	t	•	t	t	•	•
goethite	•	•	•	t	t	t	•

*t = trace amount, • = none

Table 2. Chemical Analyses of Plagioclase (weight percent).

	gneiss (B1g)			garnet granofels (B2)						
an. no.	1	2	3	4	5	6	7	8	9	10
SiO_2	64.26	62.83	62.62	55.62	56.56	55.83	55.85	57.12	56.24	56.26
Al_2O_3	23.36	23.06	23.08	26.99	26.76	26.91	27.03	26.97	27.06	27.58
Fe_2O_3	0.01	0.00	0.10	0.01	0.00	0.01	0.00	0.01	0.01	0.01
CaO	4.21	4.06	4.10	8.97	8.54	8.69	8.65	8.75	9.00	9.39
Na_2O	9.80	9.91	9.90	6.83	7.30	7.07	7.07	7.11	6.91	6.67
K_2O	0.04	0.07	0.04	0.04	0.02	0.02	0.01	0.01	0.04	0.04
Total	101.69	99.93	99.83	98.46	99.19	98.55	98.62	99.98	99.27	99.95

layers that extend for many meters. This contrasts with irregular, and in many places faint, compositional bands of the gneiss (Gn), and the more well-defined foliation of the mylonite series gneisses (MyGn, Pmy, and My). The modal compositions of stratiform mylonitic gneiss (SMyGn) are similar to the gneiss (Gn) (Table 1), although the light colored layers may be higher in quartz and in some cases richer in potassium feldspar (≥ 30% by volume). The texture of the stratiform mylonitic gneiss is somewhat similar in appearance to the "pinstriping" of the Alligator Back formation described by Rankin and others (1973).

Amphibolites (Am) in the Beaucatcher cut occur in lenses or discontinuous layers, with margins subparallel but locally discordant to the foliation. One major layer is parallel to the foliation. Most of the amphibolites are strongly schistose and contain hornblende as the princi-

Table 3. Chemical Analyses of Garnets (weight percent).

	gneiss (B1g)							garnet granofels (B2)				
loc'n.	rims				centers			rims			centers	
an. no.	2	3	4	6	1	5	7	8	10	12	9	11
SiO_2	37.04	37.00	37.39	36.56	36.98	35.87	36.01	37.75	37.90	37.73	36.60	37.95
TiO_2	0.03	0.02	0.01	0.04	0.02	0.02	0.03	0.05	0.03	0.00	0.02	0.01
Al_2O_3	21.07	20.87	21.43	20.93	20.87	20.54	20.86	21.43	21.36	21.31	21.01	21.50
FeO	31.18	30.86	28.56	31.96	30.77	31.64	31.47	29.89	28.08	30.27	28.22	28.98
MnO	4.91	4.58	1.11	3.74	4.89	4.81	4.80	0.88	0.93	1.04	0.89	1.08
MgO	2.71	2.77	7.65	3.28	2.64	2.66	2.75	5.89	6.12	5.12	7.22	6.33
CaO	0.99	0.98	1.04	1.04	0.97	1.06	1.13	2.01	2.68	2.25	2.17	2.30
Total	97.94	97.08	97.19	97.55	97.13	96.60	97.05	97.90	97.10	97.72	96.13	98.15

Figure 4. Stratiform mylonitic gneiss in (a) hand specimen and (b) micrograph, with same mineral composition as common gneiss but annealed texture and pronounced layering. Lens cap in (a) is 6 cm in diameter; long dimension of micrograph is 1 mm.

pal amphibole. Modally, 50% or more of the typical rock is hornblende (Table 1), and it commonly defines a lineation (Figure 5). Most of the amphibolites are fine-grained (0.5 - 1.0 mm), but some show a coarse (≥ 5 mm) granoblastic texture. Some amphibolites, designated porphyroblastic amphibolites (PAm), display hornblende porphyroblasts in a matrix dominated by hornblende and plagioclase. The plagioclase in amphibolites ranges from An_{29} to An_{47}, which is more calcic than plagioclase in any other rocks in the cut. Garnet makes up a significant percentage of many amphibolites and comprises over 25% in one amphibolite on the northeast side of the road cut. Minor minerals include biotite and apatite, and traces of zircon and calcite.

Garnet granofels (GGf) and garnet biotite schist (GBSch) differ only in the relative percentages of the constituent minerals (Table 1) and typically are found in close association with one another. Both contain major amounts of al-

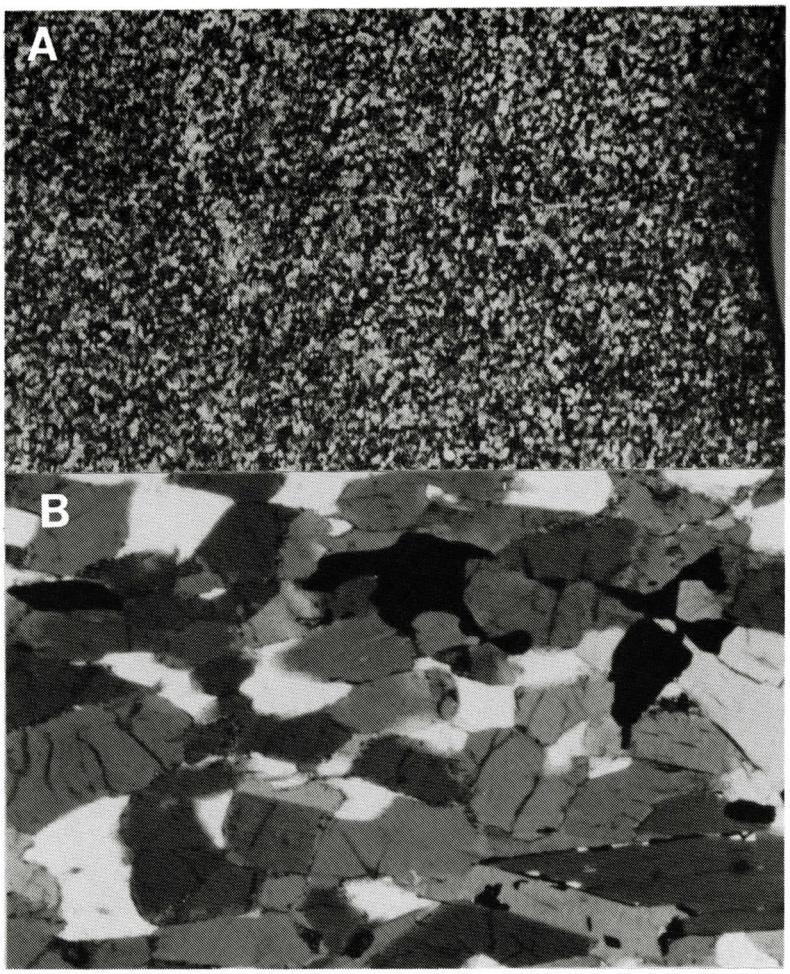

Figure 5. Hornblende amphibolite in (a) hand specimen and (b) micrograph. Edge of lens cap is at right of hand specimen photo. Lens cap in (a) is 6 cm in diameter; long dimension of micrograph is 1.1 mm.

mandine garnet and andesine (Figure 6; Tables 2, 3). However, garnet biotite schist has approximately ten percent each of biotite and sillimanite, whereas garnet granofels has only two percent of each and a greater percentage of garnets. Greater amounts of biotite define the schistosity in the garnet biotite schist. Garnets in the garnet granofels and garnet biotite schist tend to be richer in magnesium and calcium, and poorer in manganese than garnets from the gneiss (Table 3).

In thin sections B2 (GGf) and B12 (GB-Sch), garnet is rimmed by sillimanite. In B12, kyanite is rimmed by sillimanite, which indicates that sillimanite crystallized at a later stage than kyanite did. Chlorite appears in B2 but probably formed following peak metamorphism (see the discussion under METAMORPHISM). The garnet-biotite schist has approximately five percent microcline, and both garnet-rich rocks contain small amounts of sphene, zircon, apatite, and calcite.

Amphibole-biotite granofels (ABGf) is found as thin layers (< 1 m) in two places in the road cut. The major mineral in this rock is plagioclase (andesine), accompanied by minor amounts of biotite, chlorite, hornblende, and cummingtonite. Hornblende, cummingtonite, and chlorite tend to be grouped together, suggesting formation from a common phase. In

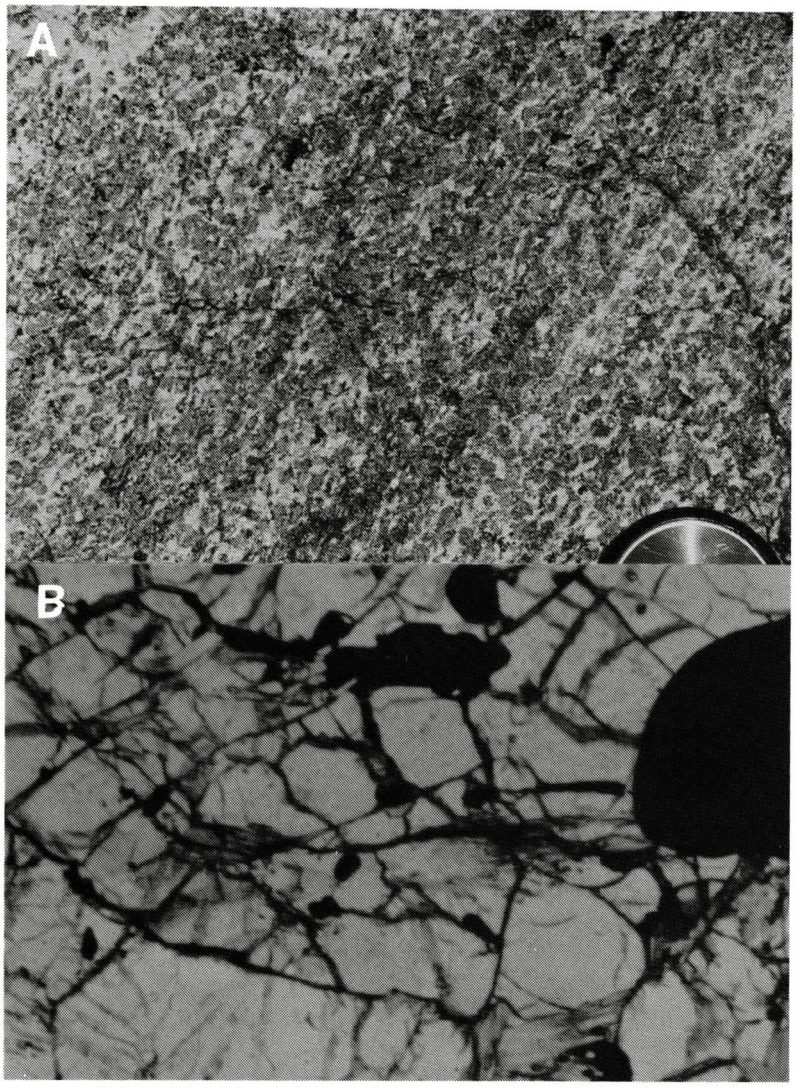

Figure 6. Garnet granofels in (a) hand specimen and (b) micrograph. Most of the discrete darker grains are garnets. Lens cap in (a) is 6 cm in diameter; long dimension of micrograph is 1.1 mm.

view of the paragenetic position of chlorite in other sections and the cross-cutting nature in this section, the chlorite probably is a later-formed phase. Some of the hornblende and cummingtonite are apparently unaltered, but some cummingtonite appears to be rimmed by hornblende. The only trace minerals in this rock are apatite and calcite.

Several variations of schist occur in the road cut, including biotite muscovite schist (BMSch), muscovite biotite garnet schist (MBGSch), and actinolite schist (ActSch). Muscovite biotite garnet schist occurs sporadically in layers ≤ 1 m thick through the road cut, whereas biotite muscovite schist is widespread but occurs in layers ≤ 2 cm. Actinolite schist is found in only one layer, a few meters thick, on both sides of the cut (Figure 2). The actinolite schist contains actinolite and chlorite as well as abundant pyrite, with a few crystals as large as a centimeter across (Table 1).

Feldspathic layers that resemble granitoid

pegmatites with coarsely crystalline white feldspar and quartz are common throughout the cut. These pegmatite-like layers (Peg) are centimeters to several meters across. They range from tabular to pinch and swell layers, and they parallel and cut across the foliation. A complete gradation seems to exist between mylonitic rocks that contain rounded, relatively isolated feldspars on one end of the spectrum, and pegmatite-like layers composed almost entirely of feldspar at the other.

Opaque Minerals

Opaque minerals are remarkably consistent in abundance throughout the cut. Overall, opaque grains are finely disseminated, usually one millimeter or less in length, and make up three percent or less of the total rock volumes. The only exception is the occurrence of large pyrite cubes in the actinolite-chlorite schist.

Ilmenite is by far the most common oxide, with rutile widespread but abundant only in the garnet granofels and garnet-biotite schist. Ilmenite, rutile, and magnetite tend to concentrate in biotite and chlorite but also are scattered within and among the other minerals. Ilmenite forms rounded and subhedral platelets, whereas rutile is included as lamellae in ilmenite or as discrete rounded and elongate grains. In some cases, rutile grains are rimmed by ilmenite. Magnetite appears uncommonly and only in small amounts. Hematite and goethite occur sporadically in trace amounts and appear to be oxidation products of pyrrhotite.

Sulfide minerals have been weathered extensively in most outcrops in the Asheville quadrangle but are widely disseminated and visible in some places on the road cut. Pyrrhotite is most abundant and occurs as irregular grains scattered among silicate minerals and in some places within biotite and chlorite. Lesser amounts of chalcopyrite occur primarily as rounded and irregular inclusions in pyrrhotite, but also as individual grains. Trace amounts of pentlandite occur as typical flame-shaped inclusions in pyrrhotite in the amphibolites, granofelses, and the garnet-biotite schist.

METAMORPHISM

Classic indicator minerals and mineral assemblages for the sillimanite zone of the upper-amphibolite facies for pelitic and mafic rocks are prevalent in the Beaucatcher cut. This facies corresponds to medium grade metamorphism of Winkler (1979, ch. 14). Indicator minerals include sillimanite for the gneisses (metagraywackes), and hornblende + plagioclase ($An_{>20}$) ± almandine for the mafic rocks (Turner, 1981; p. 209 & 366). The assignment of these rocks to the sillimanite zone of the amphibolite facies agrees with that of Carpenter (1970), who based his analysis on heavy mineral stream sediments in the Blue Ridge. Butler (1973) assigned the AMS to the sillimanite zone also, in his study of deformation and metamorphism in the Spruce Pine synclinorium, north and east of the Beaucatcher cut. Mafic rocks of the Ashe were further classified according to the CFM projection (Abbott, 1982), which evolved from the AFM diagram (Thompson, 1957) for metapelites. The mafic rocks found in the Beaucatcher cut fit subfacies 7 or 9 of the amphibolite facies, based on the occurrence of hornblende + garnet ± epidote ± biotite, in the presence of quartz + magnetite + plagioclase ± K-feldspar.

These classic Barrovian minerals of the AMS represent the medium pressure/temperature type progressive regional metamorphism (facies series) of Miyashiro (1975, p. 73; 1994, p. 207). The staurolite zone occurs in the western part of the Asheville 7.5 minute quadrangle (Miller, J.W. and Fryer, K.H., unpublished data) and the sillimanite-muscovite zone exists at the Beaucatcher cut and eastern part of the quadrangle. The sillimanite zone of metamorphism trends southwest into Georgia and northeast, near Celo, North Carolina (Carpenter, 1970). It occurs again in the vicinity of Stuart, Virginia (Rankin and others, 1973). Elsewhere, the AMS shows garnet to kyanite grade metamorphism (Rankin and others, 1973; Abbott and Raymond, 1984), with the exception of granulite facies metamorphism reported in the Chunky Gal Mountain mafic-ultramafic com-

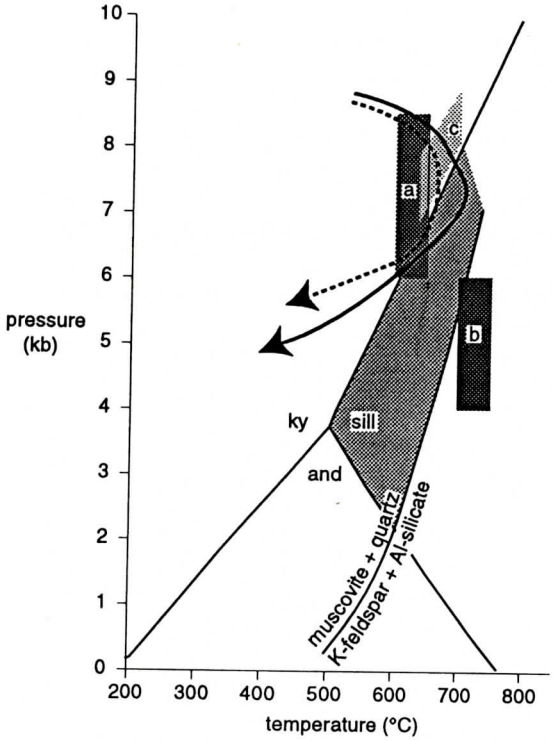

Figure 7. Metamorphic conditions and possible P-T paths of pelitic mineral assemblages at the Beaucatcher cut. The aluminosilicate triple point is from Holdaway and Mukhopadhyay (1993), and the muscovite-disappearance curve is from Evans (1965), Chatterjee and Johannes (1974), Helgeson and others (1978), and Turner (1981). Peak or near-peak conditions at the Beaucatcher cut occurred within the medium-shaded region where sillimanite and muscovite + quartz are stable. Peak metamorphic conditions are shown for the region near Boone (a - McSween and others, 1989) and the Chunky Gal Mountain complex (b - McElhaney and McSween, 1983). Metamorphic stability field is shown for north of Burnsville (c - Goldberg and others, 1992).

plex in North Carolina, near the Georgia border (McElhaney and McSween, 1983). Eclogite facies metamorphism also may occur in an eclogite at the AMS-basement contact north of Burnsville, North Carolina (Willard, 1994; Willard and Adams, 1994; Adams and others, 1995).

The appearance of sillimanite forms a minimum boundary (from Holdaway and Mukhopadhyay, 1993), and the reaction curve for the disappearance of muscovite (Evans, 1965; Chatterjee and Johannes, 1974; and Helgeson and others, 1978; Turner, 1981) forms a maximum boundary for peak or near-peak metamorphic conditions at the Beaucatcher cut (Figure 7). However, these boundaries should be regarded as regions rather than sharp boundaries because of possible complicating factors. Most natural chemical systems are much more complex than experimental ones, and slight changes in physicochemical situations can significantly shift reaction curves. For example, muscovite does not disappear when $P_{H_2O} > 3.5$ kb; under those conditions, anatexis indicates the beginning of high-grade metamorphism (Winkler, 1979). Peak metamorphism almost certainly exceeded 3.5 kb at the Beaucatcher cut if only because of the existence of sillimanite with indications of amphibolite facies metamorphism. Newton (1966) and Turner (1981) indicated 4 - 6 kb and 500° to 600°C for the conditions of the classical sillimanite isograd, and Barker (1983) gave values of 6 - 9 kb from middle amphibolite to granulite facies. This realm of metamorphism should occur at a depth of 10 - 20 km, where it is assumed that $P_{fluid} = P_{load}$. To date however, no work has been done on the composition of the fluid that existed in the AMS during peak metamorphism. The widespread occurrence of pyrrhotite throughout the cut indicates that $P_{H_2O} < P_{fluid}$ (Guidotti, 1970). While some textures and structures at the Beaucatcher cut appear to be caused by migmatization, such as the remobilization of feldspars and quartz into pegmatitic layers, there is no other evidence of anatexis. Therefore, peak or near-peak metamorphic conditions at the Beaucatcher cut likely occurred within the vicinity of the medium-shaded region of Figure 7.

Peak metamorphic conditions were estimated with mineral exchange geothermometers and geobarometers to be 725 ± 25°C and 4 - 6 kb in the Chunky Gal Mountain complex of the AMS southwest of Asheville (McElhaney and McSween, 1983). Peak metamorphism northeast of Asheville, near Boone, North Carolina was estimated at 700°C and > 7 kb using petrogenetic reactions (Abbott and Raymond, 1984).

Subsequently, conditions were refined to 600-650°C and 7.5 kb on the basis of mineral exchange geothermometers and a barometer (McSween and others, 1989; Figure 7). Kyanite but not sillimanite is found in the study area near Boone. Sillimanite occurs only along grain boundaries of other minerals, just north of Burnsville (Goldberg and others, 1992), implying the growth of sillimanite subsequent to the peak of metamorphism. Sillimanite occurs along grain boundaries and throughout grains of kyanite, garnet and other minerals at the Beaucatcher cut, which indicates fibrous sillimanite followed kyanite. Metamorphic conditions at the Beaucatcher cut were probably intermediate between those estimated by McSween and others (1989) and McElhaney and McSween (1983), and perhaps within those estimated by Goldberg and others (1992). Sillimanite was produced near the peak of prograde metamorphic conditions or soon thereafter, with a drop in pressure during retrogressive metamorphism. Two of these possible paths of metamorphism are shown in Figure 7, modeled after typical examples in Miyashiro (1994, p. 33). The solid P-T path would likely produce sillimanite during prograde metamorphism, and the dotted P-T path could produce sillimanite during retrogressive metamorphism.

The time of peak metamorphism has been estimated to be 320 to 430 Ma (Carpenter, 1970; Butler, 1973; Rankin and others, 1973; Hatcher, 1978; and Abbott and Raymond, 1984), based on isotopic geochemistry and stratigraphy. More recent preliminary estimates, based on samarium-neodymium whole-rock ages from eclogites in the AMS southwest of the Grandfather Mountain window, are approximately 410 - 450 Ma (Adams and others, 1995). Abbott and Raymond (1984) discerned four metamorphic events, with peak metamorphism occurring during the Taconic Orogeny. They designated M1 as a pre-Taconic recrystallization event which affected ultramafic rocks, and M2 as the peak metamorphic event which affected all rock types during the Taconic Orogeny. The latter event was synchronous with isoclinal folding (Butler, 1973) and produced the amphibolite facies assemblages (M1 of Butler (1973) = M2 of Abbott and Raymond (1984)). An M3 event attributed to the Acadian orogeny was marked by emplacement of granitoid plutons of the Spruce Pine Plutonic Suite (Butler, 1973; McSween and others, 1991), and the growth of talc and anthophyllite in ultramafic rocks (Abbott and Raymond, 1984). The Alleghenian M4 event is indicated by saussuritization of plagioclase, replacement of kyanite and microcline by white mica in pelitic rocks (Butler, 1973), and by the growth of serpentine in ultramafic rocks (Abbott and Raymond, 1984). The growth of chlorite was indicated by Butler (1973) in M3 and by Abbott and Raymond (1984) in both M3 and M4. Because only felsic and mafic rocks occur in the Beaucatcher cut, M1 is not discernible. M2 is indicated at the cut by the upper Amphibolite facies mineral assemblages, including kyanite and sillimanite. The final metamorphic mineral growth phase is the growth of chlorite, especially as a replacement of garnet. This represents a retrograde event that may correlate with M3 and/or M4 of Abbott and Raymond (1984).

PROTOLITHS

Rocks of the Ashe Metamorphic Suite were first described by Keith (1903), who named the Carolina and Roan gneisses but did not speculate on the nature of the protolith. As a result of studying ore deposits in the Blue Ridge, Weed and Watson (1906) recognized that the wall rocks of the Great Gossan Lead, a series of massive sulfide lenses in the AMS, are "in part altered sediments and in part igneous masses of basic and acid types, principally the former."

Gneiss is the most common rock type at the Beaucatcher cut and throughout the Asheville 7.5 minute quadrangle. Most workers (e.g. Rankin, 1970; Rankin and others, 1973; Abbott and Raymond, 1984; and Gair and Slack, 1984) agreed that this gneiss represents graywacke with other interbedded metasedimentary rocks. Abbott and Raymond (1984) and Rankin (1970)

Table 4. Chemical Analyses of Silicic and Intermediate Rocks*.

	ave. sandst.	light SMyGn	med SMyGn	dark SMyGn	typical rhyol.	Gn	Gn	Gn	MyGn	typical gywk	typical shale
		B171	B166	B165		B1	B109	B273	B236		
SiO_2	78.33	81.1	83.1	71.1	72.82	74.76	73.1	72.1	65.1	64.7	58.10
TiO_2	0.25	0.23	0.48	0.73	0.28	0.78	0.83	0.76	1.21	0.5	0.65
Al_2O_3	4.77	8.18	6.25	11.5	13.27	9.91	10.8	11.1	15.6	14.8	15.4
Fe_2O_3	1.07	1.23	2.91	5.74	1.48	4.04	4.89	4.43	8.02	1.5	4.02
FeO	0.30				1.11					3.9	2.45
MnO		<0.03	<0.03	0.13	0.06	0.04	0.08	0.06	0.15	0.1	
MgO	1.16	0.58	1.23	2.28	0.39	1.29	1.28	1.08	2.29	2.2	2.44
CaO	5.50	0.31	0.75	1.25	1.14	1.18	1.32	1.58	1.94	3.1	3.44
BaO	0.05					0.04					0.05
Na_2O	0.45	0.78	1.03	1.20	3.55	2.81	3.54	1.74	2.71	3.1	1.30
K_2O	1.31	6.06	2.30	3.44	4.30	1.19	1.35	3.44	2.27	1.9	3.24
H_2O	1.63				1.41					3.1	5.00
P_2O_5	0.08				0.07	0.09				0.2	0.17
CO_2	5.03				0.08					1.3	2.64
SO_3	0.07									0.4	0.64
LOI		0.70	0.77	1.87		0.06	0.79	2.78	1.21		
Total	100.0	99.20	98.85	99.24	99.96	96.19	97.88	99.07	100.5	100.8	99.53

*Average sandstone (sandst.), typical graywacke (gywk.), and typical shale analyses from Pettijohn (1957); typical rhyolite (rhyol.) analysis from Cox et al. (1979).

recognized the interbedded mica schists as metashales, and Gair and Slack (1984) indicated that meta-arkose was found with the graywacke. Nearly all the gneisses at the Beaucatcher cut, including the stratiform mylonitic gneiss, have bulk compositions that fall between graywacke and other sandstones (Table 4). Conceivably, some of the potassium-rich gneisses could be interbedded meta-rhyolites, but there is no textural evidence at the cut to support that hypothesis. Rankin and others (1973) found no evidence of felsic or intermediate metavolcanic rocks to the northeast. However, Merschat and Wiener (1990) suggested that felsic pyroclastic material may occur in the AMS within the Asheville and several nearby quadrangles. They base their assertion on modal analyses, in which the felsic volcanics could be represented by felsic gneisses with high plagioclase, low quartz, and little or no potassium feldspar.

On the basis of relict features, Rankin (1970) and later Rankin and others (1973) interpreted the finer and coarser grained amphibolites as metabasalts and metagabbros, respectively. Some of the thin layers (~ 1 cm) of amphibolites were interpreted as metamorphosed mafic tuffs. The amphibolites at the Beaucatcher cut contain mainly hornblende and plagioclase (An_{29} - An_{47}) ± garnet (almandine) (Table 5). They have finely (~0.5 - 1.0 mm) and coarsely crystalline (≤ 7 mm across) textures, and a locally porphyroblastic texture containing both finely and coarsely crystalline hornblende. If the amphibolites have retained their relative crystallinity, as Rankin (1970) suggested, then the finer grained amphibolites at the Beaucatcher cut represent lava flows and mafic tuffs, and the coarser grained amphibolites represent intrusive rocks. The porphyroblastic amphibolites possess the same mineralogy as the fine and coarse variations but have coarse (~ 5 mm) hornblende crystals in addition to fine crystals. These textures may represent relict porphyritic texture, although Guidotti (1970) asserted that a similar bimodal texture observed in the Oquossoc area (Maine) represents two stages of growth, formed during two different metamorphic events.

Bottino (1971) corroborated the interpretation of a mafic origin for AMS amphibolites by showing that the Rb/Sr signatures were similar to those in basaltic rocks. Bryant and Reed (1970) and subsequently Abbott and Raymond (1984) found that the whole rock composition of the amphibolites indicated a metabasaltic protolith. Gair and Slack (1984) used major and minor element geochemistry to further categorize the amphibolites around the Great Gossan Lead as low-titanium (Ti) tholeiitic basalt.

Table 5. Chemical Analyses of Mafic Rocks*.

	typical						MBG	GB	ave.
	basalt	Am	Am	PAm	GGf	ActSch	Sch	Sch	dunite
		B8b	B85	B80	B2	B345	B72	B396	
SiO_2	49.20	46.37	45.2	44.1	47.26	49.0	40.1	37.2	38.29
TiO_2	1.84	2.35	2.37	0.71	1.09	0.76	0.97	1.61	0.09
Al_2O_3	15.74	16.18	16.3	23.6	24.50	8.92	28.3	28.3	1.82
Fe_2O_3	3.79	13.74	15.41	10.2	16.21	8.28	13.4	17.0	3.59
FeO	7.13								9.38
MnO	0.20	0.26	0.36	0.11	0.36	0.22	0.24	0.18	0.71
MgO	6.73	6.83	6.79	4.78	4.32	14.4	3.40	5.50	37.94
CaO	9.47	8.96	7.43	8.81	3.78	11.6	0.69	1.07	1.01
BaO		0.04			0.01				
Na_2O	2.91	3.33	3.00	3.48	1.84	1.25	1.15	1.46	0.20
K_2O	1.10	1.25	1.51	0.52	0.46	1.19	5.00	4.47	0.08
H_2O	1.38								4.84
P_2O_5	0.35	0.18			0.19				0.20
CO_2	0.11								0.43
LOI		0.86	1.55	2.15	0.99	2.66	5.15	2.65	
Total	99.95	100.4	99.92	98.46	101.0	98.28	98.40	98.99	98.58

*Typical basalt analysis from Cox et al. (1979), and average (ave.) dunite from LeMaitre (1976).

Most recently, Misra and Conte (1991) published a detailed geochemical study of the amphibolites of the AMS and Alligator Back Formation, dividing them into three groups: low-Ti (< 0.45 wt.%), intermediate-Ti (0.7-2.3 wt.%) and high-Ti (2.8-3.4 wt.%) amphibolites. Low-Ti amphibolites had very low amounts of incompatible elements and probably resulted from "mixing a depleted mid-ocean-ridge basalt (MORB) with a fluid phase enriched in light rare earth elements." Intermediate-Ti amphibolites had a geochemical similarity to N-type MORBs from a heterogeneous mantle source. High-Ti basalts had high amounts of incompatible elements and were interpreted as T-type MORBs. Intermediate-Ti amphibolites were the most prevalent type in the study area of Misra and Conte (1991), northeast of Boone. Amphibolites in the Beaucatcher cut are intermediate-Ti type also, with whole-rock compositions typical of metabasalts (Table 5).

Beaucatcher cut amphibolites tend to have Al_2O_3 content (16 wt.%) similar to those analyzed by Gair and Slack (1984) (ave. 15.2 wt.%; range 10.1-18.8 wt.%) and slightly higher than those of Misra and Conte (1991) (ave. 13.6 wt.%; range 12.07-16.20 wt.%). However, porphyroblastic amphibolite and other rocks with mafic protoliths, with the exception of actinolite schist (see below), are much higher in Al_2O_3 (24-28 wt.%). The observed composition may (1) be caused by metasomatism long after formation, (2) reflect the original composition of the magma, or (3) result from hydrothermal alteration penecontemporaneous with rock formation. Any significant chemical alteration like (1) can be ruled out, because this would have enriched the Al-rich mafic rocks as well as the other adjacent rocks, and this is not the case. The second possible explanation is that the Al-rich mafic rocks were high alumina basalts as described by Hyndman (1985), which include calc-alkaline basalts associated with andesite, dacite, and rhyolite in an arc volcanic environment. However, such associated rock types are not apparent. Some of the gneisses that now have been assigned a graywacke protolith may actually be rhyolites and dacites, although no textural evidence for this exists. Similarly, there is no hint of associated andesites. Thus, with little or no evidence for a volcanic arc-type sequence of rocks, a lack of other igneous analogs having similar composition, and the restriction of Al-enrichment to certain rock types, (3)

penecontemporaneous hydrothermal alteration seems to be the most plausible mode of formation of the high-alumina rocks. This does not conflict with, and may support, the work of Misra and Conte (1991), which indicated that the intermediate-Ti amphibolites, including amphibolites of Gair and Slack (1984), are ocean floor basalts rather than low-K tholeiites found at convergent plate boundaries. They based their conclusion on Ti-Cr, TiO_2-Zr, and TiO_2 versus CaO/TiO_2 and Al_2O_3/TiO_2 variation diagrams. The Beaucatcher mafic rocks fall within the mid-ocean ridge basalt range shown by Misra and Conte (1991) in the TiO_2 versus CaO/TiO_2 and $Al2O_3/TiO_2$ variation diagrams, although the Al_2O_3/TiO_2 values are ambiguous for the porphyroblastic amphibolite and mica-garnet schist.

Other common rock types that apparently have mafic protoliths are the garnet granofels, garnet biotite schist, and actinolite-chlorite schist. These all have whole-rock compositions similar to basalts (Table 5) but with some variation, especially for aluminum and iron contents. The occurrence of pentlandite further indicates a mafic or ultramafic protolith. Pentlandite is found in all mafic rocks of the Beaucatcher cut except actinolite schist (Table 1).

The medium- to coarse-grained actinolite schist contains primarily actinolite, with varying amounts of chlorite (Table 1). This is the only rock in the Beaucatcher cut in which pyrite (cubes up to 1.5 cm across) occurs rather than pyrrhotite. In the AMS host rocks of the Great Gossan Lead, Gair and Slack (1984) reported a similar lithology (actinolite-chlorite schist) with a high MgO content (17.7 wt.%), for which they suggested an intrusive origin of a picrite-like basalt. Actinolite schist at the Beaucatcher cut has a similar whole rock composition, so a mafic igneous origin would be reasonable. Pentlandite occurs in rocks with mafic protoliths at the Beaucatcher cut and adds evidence for a mafic (or ultramafic) origin in rocks with ambiguous rock compositions but does not occur in the actinolite schist. Pyrrhotite and chalcopyrite do not occur in the actinolite schist, so pentlandite cannot be expected to occur without the typical host minerals (Ramdohr, 1980). The actinolite schist occurs as one foliation-parallel layer on both sides of the Beaucatcher cut. This suggests the geometry of a lava flow or a sill.

The garnet granofels and garnet-biotite schist are similar, except that the schist contains more biotite (10% in GBSch and 2% in GGf) and iron oxide and less silica (Table 5). The two rock types are found together, with contacts parallel to the foliation on both sides of the cut on the west end (Figure 2). The occurrence of pentlandite in both rocks indicates a mafic or ultramafic protolith, an interpretation that is reinforced by the low silica content (Table 5). This suggests that these rocks originated as a mafic or ultramafic sill or lava flow that likely was affected by penecontemporaneous hydrothermal alteration.

Amphibolites of the Ashe Metamorphic Suite northeast of Boone contain minor layers enriched in quartz and epidote or garnet, with the garnet amphibolites containing $\leq 50\%$ (modal) garnet (Abbott and Raymond, 1984). Abbott and Raymond's (1984) assertions that these protoliths were metabasalts parallels our assignment of a mafic igneous protolith to the Beaucatcher garnet-rich rocks. The mineralogy of the garnet amphibolites they describe is similar to that of the Beaucatcher garnet granofels and garnet-biotite schist.

The mineral composition of garnet-rich rocks at the Gossan Lead also is similar to that of the garnet-rich rocks at the Beaucatcher cut. The Gossan Lead "spessartine-rich rocks" contain "minor to subequal amounts of chlorite, quartz, plagioclase, or biotite" (Gair and Slack, 1984), whereas the Beaucatcher garnet granofels contains primarily almandine garnet and plagioclase, with other minor minerals (Table 1). However, the bulk chemical compositions seem to be significantly different. The Gossan Lead garnet-rich rocks are much lower in Al_2O_3 and much higher in SiO_2 and MnO. These rocks apparently lack pentlandite, but contain pyrrhotite. The garnets at the Gossan Lead are much richer in MnO (20-23 weight%) than the Beaucatcher garnets (Table 3). Gair and Slack (1984)

did not speculate on the origin of the spessartine-rich rocks but offered several possibilities for protoliths from other occurrences. Swanson and Raymond (1977) suggested manganiferous chert and oceanic crust as protoliths. Considering the bulk composition and absence of pentlandite, the origin of the Gossan Lead garnet-rocks probably differed from that of the Beaucatcher cut rocks.

The pegmatitic layers are composed entirely of feldspar and quartz. They occur irregularly throughout the Beaucatcher cut as concordant or discordant layers, or as lenses. The pegmatitic lenses are commonly, but not necessarily, found in the noses of folds. Sizes of the layers or lenses may range from centimeters to several meters across. Stose and Stose (1957) noticed rocks like these that were "sheared out" in the correlative Lynchburg Formation in Virginia. Carpenter (1970) noted that these layers in the AMS might be caused by anatexis or metamorphic differentiation. This conclusion appears to be reasonable because the Beaucatcher rocks should have been close to or reached the point of high grade/upper amphibolite facies metamorphism, where migmatization begins (Winkler, 1979). Further, the composition of the pegmatitic layers fits that of a migmatite.

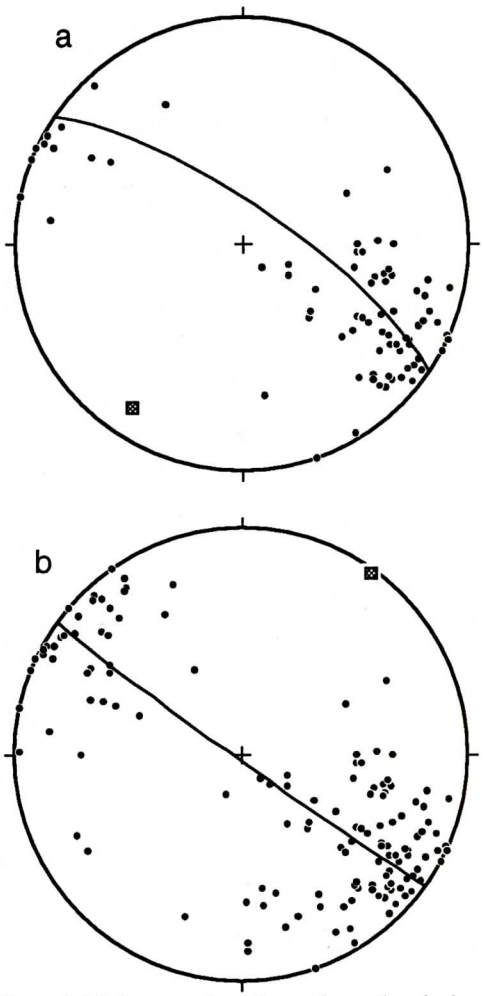

Figure 8. Pi diagrams (equal area, lower hemisphere projection) for the Beaucatcher cut (a) and for a traverse across the northern Asheville 7.5 minute quadrangle which includes the Beaucatcher data (b). N = 76 and 141, respectively. Dots = poles to foliation /schistosity; box = calculated fold axis.

STRUCTURE

Foliation and schistosity are predominantly moderately to steeply northwest-dipping at the Beaucatcher cut, although high southeast dips also are present (Figure 8a). The calculated best-fit great circle to these Beaucatcher data plotted with data from an east-west traverse across the Asheville 7.5 minute quadrangle (Miller and Fryer, 1992), provides a calculated fold axis of 036/02 for a major fold of the foliation (Figure 8b). While regional cylindricity is unlikely, fieldwork elsewhere in the quadrangle demonstrates consistency of axis trend (NE), and sub-horizontal plunge. Lineations visible on some foliation surfaces exhibit low plunges to the northeast and south-southwest (Figure 9a). The actinolite layer and biotite-kyanite schist are distinctive in exhibiting lineations with moderate plunge to the northwest; lineations elsewhere in the quadrangle are confined to low plunges to the northeast and southwest to south. The mylonitic gneiss does not show a lineation readily in outcrop, but samples sawn parallel to foliation revealed strike-parallel mineral elongation lineations.

A variety of fold styles is evident at Beaucatcher Mountain. Three dimensional exposure of fold forms is rare in the cut; however, one set

of fold axes appears to group sub-parallel to the northeast trending lineations (Figure 9b). Work on this aspect of the cut continues. A description of fold styles and approximate average attitudes follows.

Isoclinal intrafolial folds are common within the gneiss. Tight asymmetrical folds of gneissic foliation plunge shallowly to the northeast to north-northeast. Chevron folds in stratiform mylonitic gneiss plunge steeply to the northeast. Interference fold patterns and possible sheath folds are visible on some outcrop surfaces. Pegmatitic veins are folded ptygmatically within fine-grained gray gneiss. Pegmatite boudins also occur within the gray gneiss and are truncated locally by small shear zones. Discrete mylonite zones within the gneiss contain sigmoidal porphyroclasts.

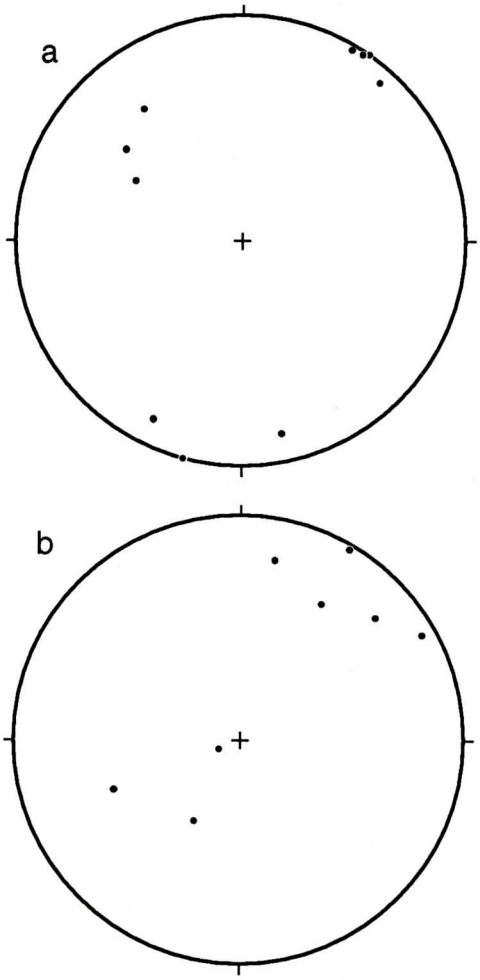

Figure 9. Lineation data (equal area, lower hemisphere projection) (a) and fold axis data (b), for the Beaucatcher cut and quadrangle traverse. N = 10 and 8, respectively.

Petrographic study of selected thin sections from Beaucatcher Mountain indicate that deformation continued after peak metamorphic conditions. While sections from the stratiform mylonitic gneiss demonstrate annealed fabrics, sections from schist layers and from mylonitic gneiss are annealed partially or not at all. Large feldspar grains in the gneiss and schist exhibit undulose extinction with recrystallization confined to narrow mantles, sigmoidal tails, or grain boundaries in felsic lenses or layers. Small recrystallized feldspar and quartz grains also are undulose, indicating that strain continued to accumulate during recrystallization.

A sample of biotite kyanite schist contains two foliations with characteristic S-C fabric relationship (Simpson and Schmid, 1983). The S-surfaces are defined by relatively large grains of biotite and kyanite. The narrow, through-going C-surfaces are defined by elongate biotite grains and small kyanite grains, with the S-surface grains curving into the C-surfaces (Figure 10). Lozenges of recrystallized quartz + feldspar parallel to S, have ends sigmoidal into C-surfaces. Kyanite grains are embayed by biotite and generally have ragged margins. Sense of motion indicated by these S-C fabrics is top to the southeast (lineation 312/35 in schistosity surface 188/42 W). Plagioclase twin planes are bent, and there is grain boundary recrystallization in the felsic clusters. This sample is not annealed completely, as relict plagioclase and quartz exhibit undulose extinction, and feldspar margins are embayed by metamorphic phases.

A section of mylonitic gneiss in which lineation is parallel to strike (199/55 W) exhibits an S-C fabric indicative of top to the south-southwest movement. Muscovite fish (Lister and Snoke, 1984) occur in the S-surfaces, with tails recrystallized into the through-going C-surfaces. Biotite occurs in both surfaces and is more equant in S and elongate in C. Large K-

Figure 10. Photomicrograph of biotite-kyanite schist, with s-surfaces horizontal: plagioclase + biotite + kyanite; c-surface from upper left to lower right, containing biotite + kyanite. The sense of shear in this photo is dextral, which corresponds to top-to-the-southeast motion for this sample. Crossed polars; 2.2 mm photo length.

feldspar grains have very narrow mantles of recrystallized grains, and locally exhibit patchy exsolution of plagioclase with multiple twins. Quartz layers exhibit sutured to polygonal grain boundaries, and quartz ribbons exhibit subgrain development and grain boundary recrystallization. Even the smallest recrystallized grains exhibit undulose extinction. The detailed field and petrographic study necessary for kinematic interpretation of the mylonite and shear zones continues. Once the relative timing of the deformation zones is understood, the larger issue of regional kinematic significance can be addressed.

LAYERING

According to Butler (1973), compositional layering in the AMS likely represents the original bedding. However, this relationship is not demonstrable in most places in the AMS. Various processes, such as transposition, tectonism, or igneous emplacement, could have resulted in the layers and contacts within the AMS. Lithologic contacts tend to be subparallel to foliation, as indicated by rare primary bedding plane structures near the Gossan Lead (Tso and others, 1982). Compositional layering of gneiss with schists may indicate original layering in the AMS found along the New River in Virginia (Abbott and Raymond, 1984). Intrafolial folds suggest that transposition was likely significant at the Beaucatcher cut, although some lithologic contacts are apparent.

Contacts of the major compositional layers, such as those between gneiss, amphibolites, and garnet granofels, extend for at least many tens of meters, and are mutually parallel and nearly parallel to the dominant foliation. If the dominant foliation indeed parallels original layering, as suggested by other authors studying the AMS in different locations, then the fine-grained amphibolites and garnet granofels parallel to the foliation are probably basaltic lava flows or sills. Unfortunately, relict contact

Science, v. 278, p. 389-418.
Misra, K.C., and McSween, H.Y., Jr., 1984, Mafic rocks of the southern Appalachians: A review: American Journal of Science, v. 284, p. 294-318.
Miyashiro, A., 1975, Metamorphism and Metamorphic Belts: Halsted Press, New York, 492 p.
Miyashiro, A., 1994, Metamorphic Petrology: University College London Press Limited, London, 404 p.
Newton, R.C., 1966, Some calc-silicate equilibrium relations: American Journal of Science, v. 264, p. 204-222.
Pettijohn, F.J., 1957, Sedimentary Rocks: Harper & Brothers, New York, 718 p.
Ramdohr, P., 1980, The Ore Minerals and their Intergrowths: Pergamon Press, Oxford, second ed., 1207 p.
Rankin, D.W., 1970, Stratigraphy and structure of Precambrian rocks in northwestern North Carolina, *in* Fisher, G.W., et. al., eds., Studies of Appalachian geology: central and southern: Interscience, New York, p. 227-245.
Rankin, D.W., 1975, The continental margin of eastern North America in the southern Appalachians: The opening of the proto-Atlantic Ocean: American Journal of Science, v. 275-A, p. 298-226.
Rankin, D.W., Espenshade, G.H., and Shaw, K.W., 1973, Stratigraphy and structure of the metamorphic belt in northwestern North Carolina and southwestern Virginia: a study from the Blue Ridge across the Brevard fault zone to the Sauratown mountains anticlinorium: American Journal of Science, v. 273-A, p. 1-40.
Rankin, D.W., Chiarenzelli, J.R., Drake, A.A., Jr., Goldsmith, R., Hall, L.M., Hinze, W.J., Isachsen, Y.W., Lidiak, E.G., McLelland, J., Mosher, S., Ratcliffe, N.M., Secor, D.T., Jr., and Whitney, P.R., 1993, Proterozoic rocks east and southeast of the Grenville front, *in* Reed, J.C., Bickford, M.E., Houston, R.S., Link, P.K., Rankin, D.W., Sims, P.K., and Van Schmus, W.R., eds., The Geology of North America, Precambrian: Conterminous U.S.: The Geological Society of America, v. C-2, p. 335-462.
Raymond, L.A., 1995, Petrology: Wm. C. Brown Publishers, Dubuque, IA, 742 p.
Raymond, L.A., Yurkovich, S.P., and McKinney, M., 1989, Block-in-matrix structures in the North Carolina Blue Ridge belt and their significance for the tectonic history of the southern Appalachian Orogen, *in* J.W. Horton, Jr. and N. Rast, eds., Melanges and Olistostromes of the U.S. Appalachians: Geological Society of America Special Paper 228, p. 195-215.
Simpson, C., and Schmid, S.M., 1983, An evaluation of criteria to deduce the sense of movement in sheared rocks: Geological Society of America Bulletin, v. 94, p. 1281-1288.
Stose, A.J., and Stose, G.W., 1957, Geology and mineral resources of the Gossan Lead district and adjacent areas in Virginia: Virginia Division of Mineral Resources Bulletin 72, 233 p.
Swanson, S.E. and Raymond, L.A., 1977, Origin and emplacement of Blue Ridge ultramafic rocks, southern Appalachian Mountains: Geological Society of America Abstracts with Programs, v. 9, p. 1195.
Thompson, J.B., Jr., 1957, The graphical analysis of mineral assemblages in pelitic schists: American Mineralogist, v. 42, p. 842-858.
Tso, J.L., Gilbert, M.C., and Craig, J.R., 1982, Geology of the Ashe Formation near Galax, Grayson county, SW Virginia: Geological Society of America Southeast Section Abstracts with Programs, v. 14, p. 91.
Turner, F.J., 1981, Metamorphic Petrology: Hemisphere Publishing Corporation, Washington, 524 p.
Twiss, R.J., and Moores, E.M., 1992, Structural Geology: W.H. Freeman and Company, New York, 532 p.
Urai, J.L., Means, W.D., and Lister, G.S., 1986, Dynamic recrystallization of minerals, *in* B.E. Hobbs and H.C. Heard, eds., Mineral and Rock Deformation: Laboratory Studies: Geophysical Monograph 36, p. 161-200.
Weed, W.H., and Watson, T.L., 1906, The Virginia copper deposits: Economic Geology, v. 1, p. 309-330.
Wehr, R., and Glover, L., 1985, Stratigraphy and tectonics of the Virginia-North Carolina Blue Ridge: Evolution of a Late Proterozoic hinge zone: Geological Society of America Bulletin, v. 96, p. 285-295.
Willard, R.A., 1994, Geology of the Ashe/basement contact in the areas of Burnsville and Bakersville, North Carolina: unpublished masters thesis, University of North Carolina, Chapel Hill, 54 p.
Willard, R.A., and Adams, M.G., 1994, Newly discovered eclogite in the southern Appalachian orogen, northwestern North Carolina: Earth and Planetary Science Letters, v. 123, p. 61-70.
Winkler, H.G.F., 1979, Petrogenesis of Metamorphic Rocks: Springer-Verlag, New York, 348 p.